


**AUTHOR QUERY FORM**

 <b>ELSEVIER</b>	<b>Journal:</b> PROTIS	<b>Please e-mail your responses and any corrections to:</b>
	<b>Article Number:</b> 125781	<b>E-mail:</b>

Dear Author,

Please check your proof carefully and mark all corrections at the appropriate place in the proof (e.g., by using on-screen annotation in the PDF file) or compile them in a separate list. Note: if you opt to annotate the file with software other than Adobe Reader then please also highlight the appropriate place in the PDF file. To ensure fast publication of your paper please return your corrections within 48 hours.

For correction or revision of any artwork, please consult <http://www.elsevier.com/artworkinstructions>.

Any queries or remarks that have arisen during the processing of your manuscript are listed below and highlighted by flags in the proof. Click on the ‘Q’ link to go to the location in the proof.

<b>Location in article</b>	<b>Query / Remark: <a href="#">click on the Q link to go</a> Please insert your reply or correction at the corresponding line in the proof</b>
<a href="#">Q1</a>	The author names have been tagged as given names and surnames (surnames are highlighted in teal color). Please confirm if they have been identified correctly.
<a href="#">Q2</a>	Correctly acknowledging the primary funders and grant IDs of your research is important to ensure compliance with funder policies. We could not find any acknowledgement of funding sources in your text. Is this correct?
<a href="#">Q3</a>	Please provide the valid prefix name for the object.
<a href="#">Q4</a>	The following references “Derelle et al. 2017; Riisberg et al. 2019; Ševčíková et al. 2015” are cited in the text but are missing in the reference list. Please provide the complete references or confirm if the reference citations could be deleted from the text.
<a href="#">Q5</a>	Have we correctly interpreted the following funding source(s) and country names you cited in your article: MOF; National Research Foundation of Korea; Next-generation BioGreen21 Program; Korea and National Science Foundation; National Science Foundation; UK Natural Environment Research Council; Scottish Funding Council?
<a href="#">Q6</a>	Figs. 3, 5, 9 will appear in black and white in print and in color on the web. Based on this, the respective figure captions have been updated. Please check, and correct if necessary.
	<div style="border: 1px solid black; padding: 10px; margin-top: 20px;"> <p>Please check this box or indicate your approval if you have no corrections to make to the PDF file <input type="checkbox"/></p> </div>

Thank you for your assistance.

## ORIGINAL PAPER

# Multigene Phylogeny, Morphological Observation and Re-examination of the Literature Lead to the Description of the Phaeosacciophyceae Classis Nova and Four New Species of the Heterokontophyta SI Clade

Q1 Louis Graf<sup>a</sup>, Eun Chan Yang<sup>b</sup>, Kwi Young Han<sup>a</sup>, Frithjof C. Küpper<sup>c,d</sup>,  
Kylla M. Benes<sup>e</sup>, Jason K. Oyadomari<sup>f</sup>, Roger J.H. Herbert<sup>g</sup>, Heroen Verbruggen<sup>h</sup>,  
Richard Wetherbee<sup>h</sup>, Robert A. Andersen<sup>i,1</sup>, and Hwan Su Yoon<sup>a,1</sup>

<sup>a</sup>Department of Biological Sciences, Sungkyunkwan University, Suwon 16419, Republic of Korea

<sup>b</sup>Marine Ecosystem Research Center, Korea Institute of Ocean Science and Technology, Busan 49111, Republic of Korea

<sup>c</sup>School of Biological Sciences, Cruickshank Bldg, University of Aberdeen, St. Machar Drive, Aberdeen AB24 3UU, Scotland, UK

<sup>d</sup>Marine Biodiscovery Centre, Department of Chemistry, University of Aberdeen, Aberdeen AB24 3UE, Scotland, UK

<sup>e</sup>Davidson Honors College, University of Montana, Missoula, MT 59812, USA

<sup>f</sup>Suomi College of Arts and Sciences, Finlandia University, Hancock, MI 49930, USA

<sup>g</sup>Department of Life and Environmental Sciences, Bournemouth University, Poole, Dorset BH12 5BB, UK

<sup>h</sup>School of BioSciences, University of Melbourne, Victoria 3010, Australia

<sup>i</sup>Friday Harbor Laboratories, University of Washington, Friday Harbor, WA 98250, USA

Submitted June 16, 2020; Accepted October 5, 2020

Monitoring Editor: Michael Melkonian

The relationships among the Aurearenophyceae, Phaeothamniophyceae, Phaeophyceae and Xanthophyceae lineages of the Heterokontophyta SI clade are not well known. By adding previously unexamined taxa related to these classes in a five gene phylogeny (SSU rRNA, *atpB*, *psaA*, *psaB*, *rbcL*), we recovered an assemblage of taxa previously unrecognized. We propose the class Phaeosacciophyceae class. nov., that includes *Phaeosaccion collinsii*, *Phaeosaccion multiseriatum* sp. nov., *Phaeosaccion okellyi* sp. nov., *Antarctosaccion applanatum*, *Tetrasporopsis fuscescens*, *Tetrasporopsis moei* sp. nov., and *Psammochrysis cassiotisii* gen. & sp. nov. We re-examine the literature for *Chrysoomeris*, *Nematochrysis*, *Chrysowaernella* and the invalid name “*Giraudyopsis*” and conclude

Corresponding authors.

e-mails [raa48@uw.edu](mailto:raa48@uw.edu) (R.A. Andersen), [hsyoon2011@skku.edu](mailto:hsyoon2011@skku.edu) (H.S. Yoon).

<https://doi.org/10.1016/j.protis.2020.125781>

1434-4610/© 2020 Elsevier GmbH. All rights reserved.

Please cite this article in press as: L. Graf, E.C. Yang, K.Y. Han et al.. Multigene Phylogeny, Morphological Observation and Re-examination of the Literature Lead to the Description of the Phaeosacciophyceae Classis Nova and Four New Species of the Heterokontophyta SI Clade. Protist (xxxx), <https://doi.org/10.1016/j.protis.2020.125781>

some taxa in previous studies misidentified or misnamed, i.e. *Chrysomeris* and *Chrysowaernella*, respectively. We also show that *Nematochrysis sessilis* var. *vectensis* and *Nematochrysis hieroglyphica* may belong in the recently described class Chrysoparadoxophyceae. The phylogenetic relationships of *Phaeobotrys solitaria* and *Pleurochloridella botrydiopsis* are not clearly resolved, but they branch near the Xanthophyceae. Here we describe a new class Phaeosacciophyceae, a new order Phaeosacciales, a new family Tetrasporopsidaceae, a new genus *Psammochrysis* and four new species.

**Key words:** *Chrysomeris*; Chrysoparadoxophyceae; *Nematochrysis*; Phaeosaccion; Tetrasporopsis.  
© 2020 Elsevier GmbH. All rights reserved.

## Introduction

The heterokont algae (photosynthetic stramenopiles) are an exceptionally diverse group that includes naked amoeboid organisms, flagellate and coccoid algae, silica-walled diatoms, and giant brown seaweeds. Recent phylogenetic analyses have identified three major clades, termed the SI, SII and SIII clades (Yang et al. 2012). In this paper, we focus on clade SI of photosynthetic heterokonts.

Although the flagellate class Raphidophyceae is the most deeply branching class within clade SI, the most common life forms in this clade are colonial, filamentous and thalloid algae. Historically, the identification and classification of filamentous brown algae (Phaeophyceae), yellow-green algae (Xanthophyceae) and diatoms (Bacillariophyceae) were simple and straightforward (e.g. Kjellman 1891; Pascher 1914a). Conversely, the filamentous forms classified within the Chrysophyceae (Gayral and Billard 1977a; Pascher 1914a) are now placed in other classes (e.g. Bailey et al. 1998; Graf et al. 2020; Han et al. 2018; Wetherbee et al. 2015). Convincing evidence that these “chrysophyte” filaments were unusual members of the Chrysophyceae arose from flagellar studies carried out in Gayral’s laboratory (Caen, France). Gayral’s group classified many of the marine “chrysophytes” in the order Sarcinochrysidales (Gayral and Billard 1977a,b). Subsequently, molecular phylogenetic analyses showed that the Sarcinochrysidales sensu stricto (= Sarcinochrysidaceae) belonged in the class Pelagophyceae (Saunders et al. 1997), which was classified within the heterokont clade SIII (Yang et al. 2012; Han et al. 2018). Other marine filamentous and thalloid algae classified in the Sarcinochrysidales (sensu Gayral and Billard 1977a) have been placed in the Chrysomeridophyceae (Cavalier-Smith et al. 1995), but problems exist regarding *Chrysomeris ramosa*, the type, which was never analyzed with modern methods. Furthermore, phylogenetic analyses showed that the

Chrysomeridophyceae was polyphyletic (e.g. Yang et al. 2012). In an effort to address these unresolved issues, we gathered as many of these taxa as possible for this study.

We included *Phaeosaccion collinsii* Farlow, a macroscopic sac-like alga that was described long ago from the rocky shores near Boston, Massachusetts USA, and originally classified as a brown alga (Farlow 1882). *Phaeosaccion* reaches up to 20 cm in length, the largest heterokont alga outside the Phaeophyceae. Similarly, we added *Antarctosaccion applanatum* (Gain) Delépine, a macroscopic sheet-like alga from Antarctica whose molecular phylogenetic relationship was unknown (Delépine et al. 1970; Gain 1911). *Chrysomeris* and *Nematochrysis* were described by light microscopy as uniseriate and multiseriate marine filaments (Carter 1937; Pascher 1914a,b, 1925), and additional taxa were described by light microscopy (e.g. Carter 1937; Schussnig 1940; Waern 1952). We added *Nematochrysis sessilis* var. *vectensis* from the type locality in the present analyses but we were unable to find *Chrysomeris*. Furthermore, *Chrysowaernella* and “*Giraudyopsis*” were shown to be distinctly different from the Sarcinochrysidales sensu stricto (e.g. O’Kelly 1989), but the taxonomy, nomenclature and phylogeny of these latter taxa were not fully resolved (Derelle et al. 2016; Yang et al. 2012). Finally, recent studies showed that the freshwater colonial *Tetrasporopsis* was a member of the SI clade (Stancheva et al. 2019; Yang et al. 2012), and we examined original type material to verify these results.

We sequenced the nuclear encoded small subunit ribosomal RNA (SSU rRNA) and the chloroplast-encoded *atpB*, *psaA*, *psaB* and *rbcl* genes, and we combined our results with previously published sequences to form a dataset representing all the recognized lineages of the heterokont clade SI. Here we describe a new class Phaeosacciophyceae, a new order Phaeosacciales, a new family Tetrasporopsidaceae, a new genus *Psammochrysis* and four new species.

## Results

### Taxonomy and nomenclature

Phaeosacciophyceae R.A.Andersen,  
L.Graf & H.S.Yoon classis nov.

**Description:** Class forms a distinct lineage in molecular phylogenies of the heterokont algae; organisms unicellular, colonial, filamentous or thallic forms; cells typically with cell walls; chloroplasts one to two per cell; chloroplasts with three thylakoids per lamella plus a girdle lamella; zoospores biflagellate; anterior immature flagellum with tripartite tubular hairs; posterior flagellum smooth; eyespot frequently found in the zoospore chloroplast; flagellar apparatus similar to brown algae and xanthophyte algae.

**Type species:** *Phaeosaccion collinsii* Farlow 1882, Bull Torrey Bot. Club 9: 66.

**Lectotype specimen designated here:** FH-00870300, herbarium sheet, Farlow Herbarium of Harvard University, Cambridge, Massachusetts, USA. This specimen was collected by Frank S. Collins on 26 March 1882 from Little Nahant, Essex County, Massachusetts, USA.

Phaeosacciales R.A.Andersen, L.Graf &  
H.S.Yoon ordo nov.

**Description:** with characters of the class Phaeosacciophyceae.

**Phaeosaccioniaceae** J. Feldmann ex Gayral & Billard 1977a, *Taxon* 26:243 ('Phaeosaccioniaceae').

*Phaeosaccion multiseriatum* R.A.Andersen, L.Graf & H.S.Yoon sp. nov. (Fig. 4)

**Description:** Thallus initiated from basal cells that give rise to uniseriate filaments; mature thalli typically composed of multiseriate branched filaments, 10–20  $\mu\text{m}$  wide and up to 100  $\mu\text{m}$  long; rarely, in culture, thalli up to 800  $\mu\text{m}$  long and 150  $\mu\text{m}$  wide; cells wider than long, 4–7  $\mu\text{m}$   $\times$  3–4  $\mu\text{m}$ ; cells with a distinct cell wall; a single parietal chloroplast per cell except before cell division; a pyrenoid in the center of the plastid; few oil or chrysolaminaran vacuoles per cell; zoospores oval, approximately 4–5  $\mu\text{m}$  long and 3  $\mu\text{m}$  wide; zoospores biflagellate, flagella inserted laterally; anterior flagellum beating with a sinusoidal wave, posterior flagellum beating with a stiff sculling motion; a red eyespot present; sexual reproduction and resistant stage unknown; DNA sequences representing 18S rRNA (U78034), *atpB* (MT582089), *psaA* (HQ710646),

*psbA* (HQ710702), *psbC* (MT581965) and *rbcl* (HQ710597) are distinctive and unique.

**Holotype here designated:** cells from culture strain CCMP 1308 were preserved and mounted on a microscope slide that was deposited in the New York Botanical Garden herbarium (NY), New York City, NY USA as No. 04244501.

**Isotypes here designated:** cryopreserved culture strain CCMP 1308 deposited in the Provasoli-Guillard National Collection of Marine Algae and Microbiota, East Boothbay, ME USA; cells from culture strain CCMP 1308 were preserved and mounted on a microscope slide that was deposited in the New York Botanical Garden herbarium (NY), New York City, NY USA as No. 04244502 and deposited in the University Herbarium, University of California-Berkeley (UC), Berkeley, CA USA.

**Type locality:** San Juan Island, Washington, USA. Collected & isolated by Richard Norris.

**Etymology:** *multiseriatum* refers to many series, or filaments composed of more than one row of cells.

Authentic culture: CCMP1308.

*Phaeosaccion okellyi* R.A.Andersen, L.Graf & H.S.Yoon sp. nov. (Fig. 6)

**Description:** Thallus consisting of densely branched cells up to 300  $\mu\text{m}$  across; filament branches short, branching very frequently; cells often cuboidal or rectangular in outline, 4–7  $\mu\text{m}$  in size; cells with a distinct cell wall; single parietal chloroplast per cell except before cell division; pyrenoid in the center of the chloroplast; oil droplets and chrysolaminaran vacuoles common; zoospores biflagellate, flagella inserted laterally; anterior flagellum beating with a sinusoidal wave, posterior flagellum beating with a stiff sculling motion; sexual reproduction and resistant stage unknown; DNA sequences representing 18S rRNA (HQ710557), *psaA* (HQ710645), *psaB* (MT582027), *psbA* (HQ710701), *psbC* (HQ710755) and *rbcl* (HQ710596) are distinctive and unique.

**Holotype here designated:** cells from culture strain CCMP 1666 were preserved and mounted on a microscope slide that was deposited in the New York Botanical Garden herbarium (NY), New York City, NY USA as No. 04244503.

**Isotypes here designated:** cryopreserved culture strain CCMP 1666 deposited in the Provasoli-Guillard National Collection of Marine Algae and Microbiota, East Boothbay, ME USA; cells from culture strain CCMP 1666 were preserved and mounted on a microscope slide that was deposited in the New York Botanical Garden herbarium (NY), New York City, NY USA as No. 04244504 and



deposited in the University Herbarium, University of California-Berkeley (UC), Berkeley, CA USA.

**Type locality:** Leigh, New Zealand, near Auckland University Field Station (36.3833 S, 174.8 E). Collected and isolated by Charles O'Kelly.

**Etymology:** named in honor of Dr. Charles O'Kelly who has contributed significantly to the study of algae.

Authentic culture: CCMP1666

Family Tetrasporopsidaceae R.A.Andersen, L.Graf & H.S.Yoon fam. nov.

**Description:** Family forms a distinct lineage in molecular phylogenies of the heterokont algae; organisms unicellular or colonial; cells with distinct walls; typically one to two chloroplasts; pyrenoids common; zoospores biflagellate, flagella inserted laterally; anterior flagellum beating with a sinusoidal wave, posterior flagellum beating with a stiff sculling motion.

*Tetrasporopsis moei* R.A.Andersen & J.K.Oyadomari sp. nov. (Fig. 7).

**Description:** Cells (5-) 7–10 (-15)  $\mu\text{m}$  in diameter; each cell with two parietal plate-like chloroplasts, often lobed; no visible pyrenoid; dancing particles located between the chloroplasts; no contractile vacuole; cells forming semi-solid (or semi-hollow) colonies, thallus sometimes with gaps or perforations; new colonies formed from fragments of older colony; zoospores and sexual reproduction unknown; DNA sequences representing 18S rRNA (MT582122), *atpB* (MT582092), *psaA* (MT582061), *psaB* (MT582030), *psbA* (MT581995), *psbC* (MT581969) and *rbcL* (MT581943) are distinctive and unique.

**Holotype:** cells from culture strain A12,475 were preserved and mounted on a microscope slide that was deposited in the New York Botanical Garden herbarium (NY), New York City, NY USA as No. 04244505.

**Isotypes here designated:** cells from culture strain A12,475 were preserved and mounted on a microscope slide that was deposited in the New York Botanical Garden herbarium (NY), New York City, NY USA as No. 04244506 and deposited in the University Herbarium, University of California-Berkeley (UC), Berkeley, CA USA.

**Type locality:** a small pool, near Laurium, Michigan USA (47.2345 N 88.4260 W); sample collected on 19 June 2010. Collected by R.A. Andersen and J.K. Oyadomari, isolated by R.A. Andersen.

**Etymology:** named in honor of Dr Richard Moe, University of California-Berkeley, for his many contributions to algal taxonomy and nomenclature and his generous help to us over many years.

Authentic culture: A12,475

*Psammochrysis cassiotisii* R.Wetherbee, gen. et sp. nov. (Fig. 8)

**Description:** Cells unicellular, flattened, rounded 10–16  $\mu\text{m}$  in diameter including a cell wall, with a centrally located nucleus (Fig. 8A, B). Cells observed in pairs (i.e., daughter cells) (Fig. 8B–D). Mature cells contained two deeply lobed chloroplasts, each lobe with a pyrenoid (Fig. 8B). One chloroplast lobe contained an eyespot. Benthic cells transformed into a single, heterokont zoospore of the *Sarcinochrysis* type, 8–12  $\mu\text{m}$  in width and 16–22  $\mu\text{m}$  in length (Fig. 8E–G) with two chloroplasts, one enclosing the cell apex. Flagella inserted subapically in a depression adjacent an eyespot within the posterior chloroplast (Fig. 8F, G). Long flagellum approximately the length of the zoospore, 16–22  $\mu\text{m}$ , with tripartite, tubular hairs and directed forward, the shorter flagellum smooth, wrapped around the cell, 10–14  $\mu\text{m}$  in length. Zoospores escaped the parental wall (Fig. 8A, C, D) and were briefly motile prior to adhering to the coverslip via their two flagella, cells hovering above the coverslip. Zoospores rounded-up (Fig. 8H–J) and divided immediately (Fig. 8I–K), the daughter cells then tightly adhered to the coverslip surface adjacent to one another and flattened out. Each cell had a single, lobed chloroplast. Following zoospore release, the parental walls of the daughter cells remain as pairs (Fig. 8A, C, D). In culture, cells settled in rafts that increased in size over time, with benthic cells on the raft rim, pairs of cell wall remnants on the interior (Fig. 8C, D). Sexual reproduction was not observed. DNA sequences representing 18S rRNA (MT582121), *atpB* (MT582091), *psaA* (MT582060), *psaB* (MT582029), *psbA* (MT581994), *psbC* (MT581968) and *rbcL* (MT581942) are distinctive and unique.

**Holotype:** MELU A EC38 HONY, a mounted specimen derived from strain CS-1319.

**Type locality:** sand at the bottom of a high intertidal pool, Narooma Inlet, New South Wales 20 meters before the west entrance to the Mill Bay Boardwalk (36.20773S, 150.12512E); collected by Richard Wetherbee in April, 2015.

**Etymology:** The genus describes a sand-dwelling (Psammo-) heterokont with golden chloroplasts (i.e., -chrysis). The specific epithet honors Emmanuel Cassiotis, a legendary biology teacher, Australian naturalist and scholar, who led several expeditions to remote locations where many new taxa were found, including *Psammochrysis cassiotisii*.

**Habitat:** marine, sand-dwelling.

**Culture lodgment:** ANACC code: New South Wales strain CS-; CSIRO, Hobart, Tasmania, Australia.

***Chrysomeres ramosa*** N. Carter (1937) Arch Protistenkd 90: 49.

**Lectotype specimen designated here:** Fig. 5 of Plate 7, in Carter (1937) Arch Protistenkd 90.

### Analysis of *Tetrasporopsis fuscescens* lectotype material

To anchor the genus *Tetrasporopsis* in the phylogeny of the heterokonts, we examined a portion of the specimen of *Tetrasporopsis fuscescens* (Braun in Kützing 1849) Lemmermann collected by Braun in November 1846 and designated as the lectotype specimen (Entwistle and Andersen 1990). We obtained DNA from the rehydration of a 3 mm<sup>2</sup> piece of the lectotype material. The total DNA was sequenced by using next-generation sequencing (NGS), and after trimming and stringent quality and contamination filtration, we obtained a handful of fragments that had identity to the sequences of the *atpB* (coverage length 6.12%; identity 96.59%), *psaA* (coverage length 10.09%; identity 97.77%), *psaB* (coverage length 7.17%; identity 99.36%), *psbC* (coverage length 2.82%; identity 100%) and *rbcL* (coverage length 10.78%; identity 98.67%) genes. Phylogenetic analysis recovered monophyly of the lectotype fragments and strain SAG 20.88 with strong support (Fig. 1A–E; Supplementary Material Figs S1–S5).

### Concatenated phylogenies

A total of 105 taxa representing the recognized photosynthetic class belonging to the heterokont clade SI (i.e. Aurearenophyceae; Chrysoparadoxophyceae; Phaeophyceae; Phaeosacciophyceae, Phaeothamniophyceae; Raphidophyceae; Schizocladiphyceae and Xanthophyceae) were used to determine molecular phylogenetic relationships among those classes (Fig. 2). We used 16 taxa from the class Eustigmatophyceae (clade SII) as outgroup taxa. We generated 143 sequences of the nuclear SSU rRNA and the plastid-encoded *atpB*, *psaA*, *psaB*, *rbcL* to build a five-gene dataset along with publicly available sequences and generated 55 sequences of the plastid-encoded *psbA* and *psbC* (Supplementary Material Table S1). All new sequences were deposited in GenBank under the accession numbers MT581941–MT582138 (Supplementary Material Table S1). Taxa represented by all five genes (44; 36%), four genes (22; 18%) and three genes (44; 36%) formed the major

portion of the dataset (i.e. 90%). Only 11 taxa were represented in the concatenation by two genes.

Tree reconstructions were conducted on a concatenated five-gene DNA matrix containing 7076 nucleotides positions and a concatenated five-gene AA-SSU rRNA matrix containing 1813 amino acid positions and 1629 nucleotides positions. The trees recovered the monophyly of the SI clade (Fig. 2) with strong support [Ultrafast Bootstrap Approximation (UBA-DNA) 100%, non-parametric bootstrap (BP-DNA) 100%, UBA-AA 100%, BP-AA 100%]. Inside the SI clade, the Raphidophyceae was the first divergent lineage and was sister to the lineages traditionally composing the PX clade (UBA-DNA 100%, BP-DNA 100%, UBA-AA 100%, BP-AA 100%). Within the PX clade, three subclades were strongly recovered: (1) the Aurearenophyceae and Phaeothamniophyceae (UBA-DNA 99%, BP-DNA 94%, UBA-AA 94%, BP-AA 75%), (2) the Phaeophyceae and Schizocladiphyceae (UBA-DNA 100%, BP-DNA 100%, UBA-AA 100%, BP-AA 100%) and (3) a less supported subclade (UBA-DNA 81%, BP-DNA 50%, UBA-AA 82%, BP-AA 58%) grouping the new class Phaeosacciophyceae (UBA-DNA 100%, BP-DNA 100%, UBA-AA 100%, BP-AA 100%), the Xanthophyceae + *Phaeobotrys/Pleurochloridella* (UBA-DNA 100%, UBA-AA 100%) and the class Chrysoparadoxophyceae + *Nematochrysis* (UBA-DNA 89%, BP-DNA 70%, UBA-AA 82%, BP-AA 55%). The first two subclades were generally recovered in the five single gene trees (Supplementary Material Figs S6–S10) with no (e.g. Aurearenophyceae and Phaeothamniophyceae *psaA* tree with UBA-DNA 31%) to high support (e.g. Aurearenophyceae and Phaeothamniophyceae *rbcL* and SSU trees with UBA-DNA 95%) but not in the *psbA* and *psbC* trees (Supplementary Material Figs S11, S12). The third subclade was not recovered in any of the single gene trees, mostly because of the branching of the Chrysoparadoxophyceae (Supplementary Material Figs S6–S12). The branching among those three subclades was not supported but it appeared that the Aurearenophyceae and Phaeothamniophyceae was the first to diverge (UBA-DNA 57%, BP-DNA 28%, UBA-AA, 44%, BP-AA 15%).

Inside the class Phaeosacciophyceae, the genera *Antarctosaccion* and *Phaeosaccion* formed another monophyletic group (UBA-DNA 100%, BP-DNA 100%, UBA-AA 100%, BP-AA 100%) representing the family Phaeosaccioniaceae and the genera *Psammochrysis* and *Tetrasporopsis* formed a monophyletic group (UBA-DNA 100%, BP-DNA 100%, UBA-AA 100%, BP-AA 100%) represent-

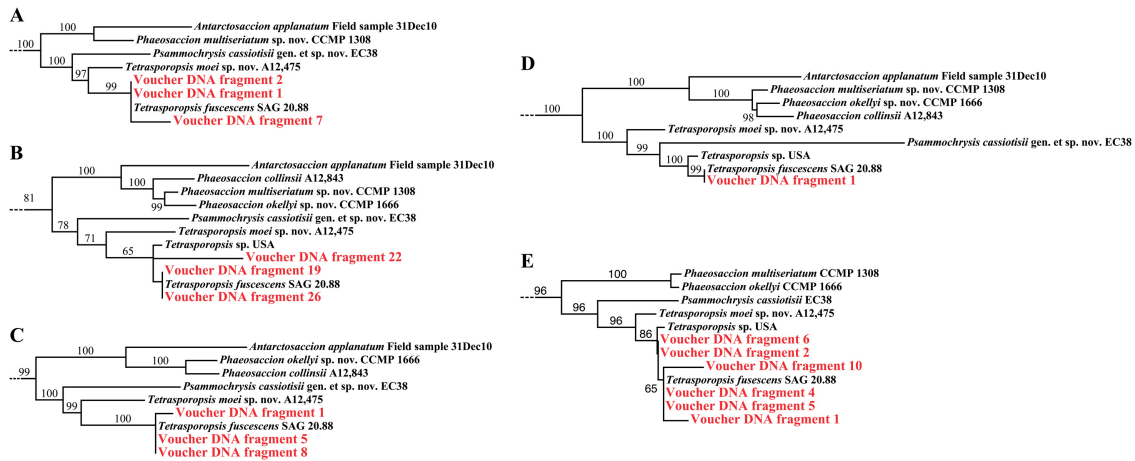


**Figure 1.** Phylogenetic positions of the *Tetrasporopsis fuscescens* lecotype genetic material within the class Phaeosacciophyceae. **A.** Maximum likelihood tree inferred with IQ-Tree v 1.6.12 with nucleotide alignments of the plastid encoded **A.** *atpB* **B.** *psaA* **C.** *psaB* **D.** *psbC* and **E.** *rbcL*. Ultrafast bootstrap approximation support values are indicated near the nodes.

ing the family Tetrasporopsidaceae (Fig. 2). These two families were consistently recovered in monophyly in the single gene trees with high support (Supplementary Material Figs S6–S12).

Within the genus *Phaeosaccion*, *P. collinsii* was the first to diverge and was sister to *P. multiseriatum* and *P. okellyi* (UBA-DNA 100%, BP-DNA 43%, UBA-AA 93%, BP-AA 46%). When all three taxa were present, this relationship was recovered in the *psaA* and *psbC* trees (Supplementary Material Figs S8 and S12) but not in the SSU tree where *P. okellyi* was the first to diverge (Supplementary Material Fig. S6).

Within the genus *Tetrasporopsis*, *T. fuscescens* and a strain isolated in California (see Stancheva et al. 2019) formed a monophyletic group and were sister to *T. moei* (UBA-DNA 100%, BP-DNA 100%, UBA-AA 100%, BP-AA 100%). When all three taxa were present, the same branching was recovered in the single gene trees with the exception of the *psbC* tree in which *Psammochrysis* branched within the genus *Tetrasporopsis* (Supplementary Material Figs S6–S12).

*Nematochrysis sessilis* var. *vectensis* strains A14,626, A14,628 and A14,479 formed a monophyletic group (UBA-DNA 100%, BP-DNA 100%, UBA-AA 99%, BP-AA 98%) and were sister to *N. hieroglyphica* (UBA-DNA 100%, BP-DNA 100%, UBA-AA 100%, BP-AA 100%) and this monophyletic genus was recovered across all the single gene trees with high support (Supplementary Material Figs S6–S12).

The tree analysis including the *psbA* and *psbC* genes recovered similar branching within the Phaeosacciophyceae but did not

recovered the monophyly of Chrysoparadoxyphyceae + *Nematochrysis* (Supplementary Material Fig. S8). Furthermore, the branching between the different subclades was different but with lower support (Supplementary Material Fig. S13).

## Morphological observations

### Phaeosacciophyceae Phaeosaccioniaceae.

*Phaeosaccion collinsii*. *Phaeosaccion collinsii* Farlow was examined using field material collected as an epiphyte on *Zostera marina* from Little Nahant, Massachusetts USA, the type locality. The thalli were macroscopic hollow tubes up to 20 cm in length (Fig. 3A, B). Each thallus was anchored by a narrow stipe (Fig. 3A, lower right corner). Cells were block-shaped, 3.5–5 μm × 4–7 μm in size (Fig. 3C). Within the thallus, cells divided in two directions and remained attached, thereby creating the hollow tubular thallus. Cell walls were clearly visible after staining with brilliant cresyl blue dye (Fig. 3D).

*Phaeosaccion multiseriatum* sp. nov. CCMP 1308. This alga produced uniseriate and multiseriate branched filaments (Fig. 4). The thallus was sometimes quite large in culture (ca. 800 μm) (Fig. 4A). Multiseriate filaments were solid, not hollow (Fig. 4B, D). Cells of the multiseriate filaments were not strictly organized, i.e. cells did not always lie in a strict directional pattern (Fig. 4C, D). At times, the cell mass appeared to be a parenchymatous mass of cells, i.e. the filamentous nature could not be discerned (Fig. 4E).



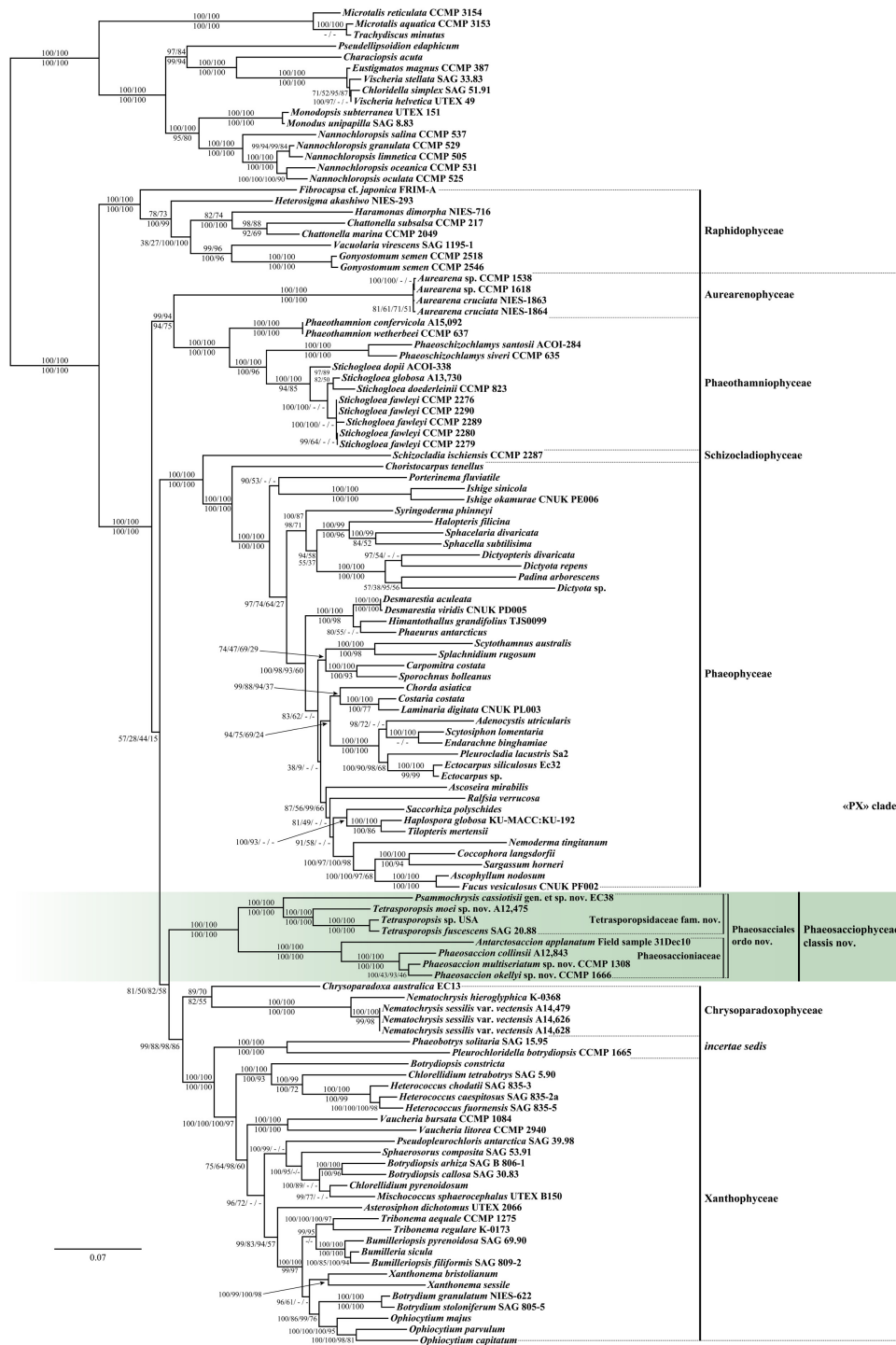


**Figure 2.** Maximum likelihood tree reconstructed from the concatenated nucleotide alignments of the plastid encoded *atpB*, *psaA*, *psaB*, *rbcl* and the nuclear encoded SSU genes. The tree was inferred with IQ-Tree v 1.6.12 using independent models for each partition. Support values are indicated near the nodes in the following order: nucleotide ultrafast bootstrap approximation/nucleotide non-parametric bootstrap/amino acid ultrafast bootstrap approximation/amino acid non-parametric bootstrap.



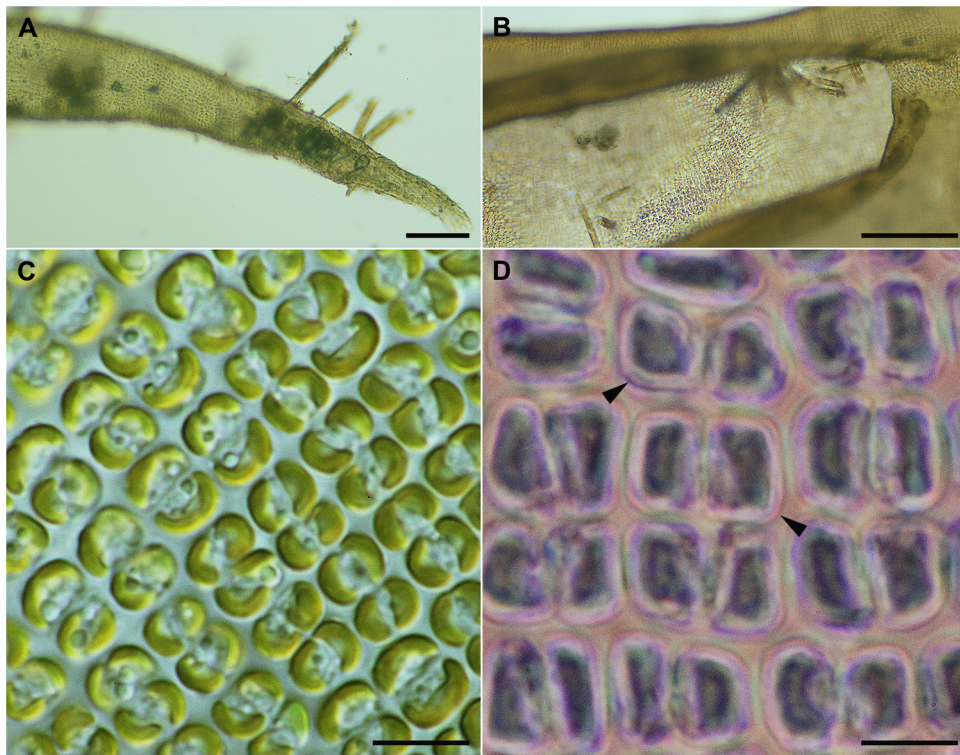


**Figure 3.** *Phaeosaccion collinsii*. **A.** Thallus showing gross morphology, with putative holdfast in the lower right corner. Note the attached diatoms. Scale bar = 100  $\mu\text{m}$ . **B.** Torn region of the thallus showing the hollow tubular gross morphology formed by a single layer of cells. Scale bar = 100  $\mu\text{m}$ . **C.** Dividing cells showing the single parietal chloroplast and the highly organized pattern. Scale bar = 10  $\mu\text{m}$ . **D.** Cells stained with brilliant cresyl blue. Note the pink-colored cell walls (arrowheads) and the lighter material between cells. Chloroplasts stained dark blue. Scale bar = 5  $\mu\text{m}$ . (For interpretation of the references to color in this figure legend, the reader is referred to the web version of this article.)

Cell division was not precise; cells divided laterally, longitudinally and diagonally (Fig. 4F–H). Cells were block-like, often shorter than wide, typically 4–7  $\mu\text{m} \times 3$ –4  $\mu\text{m}$ . Each cell had a thin cell wall (Fig. 4G, double arrowhead), and a gelatinous matrix that surrounded the filament (Fig. 4G, single arrowhead). Cells had a single parietal chloroplast (Fig. 4C, F–H). A pyrenoid was often visible in the center of the chloroplast (Fig. 4C, F, arrowheads). A few lipid droplets were present in each cell (Fig. 4F, arrow).

Zoospore formation was first signaled by the development of red eyespots on vegetative cell chloroplasts (Fig. 5A, arrowheads). The cell wall dissolved and the future zoospore was released as a spherical cell without flagella (Fig. 5B). The flagella developed and a pyriform zoospore quickly swam away (not shown). Zoospores were approximately 3  $\mu\text{m}$  wide and 5  $\mu\text{m}$  long. Zoospores were biflagellate (Fig. 5C–E). The flagella were inserted laterally, approximately 1/3 of the distance from the anterior end (Fig. 5E). The anterior flagel-

lum was approximately 1.5 times the cell length and it beat with a sinusoidal wave that pulled the zoospore forward (Fig. 5C). The posterior flagellum extended beyond the end of the cell and was approximately the length of the cell. The posterior flagellum beat with a stiff sculling motion. Upon settling, the zoospore lost its flagella and developed a gelatinous pad (Fig. 5F). Zoospores maintained an eyespot while swimming, but the eyespot was lost when the adhesion pad was formed (Fig. 5F).

*Phaeosaccion okellyi* sp. nov.. The organism was densely branched (Fig. 6A, B). In culture, flattened mats up to 125  $\mu\text{m}$  in size were produced (Fig. 6A). Most filaments were small and uniseriate (Fig. 6C, D), but mats of branched cells were sometimes multiseriate (Fig. 6B, E); parenchymatous-like thalli were not observed. Branching occurred at a high frequency, and often the first cell (i.e. settled zoospore) formed branches after only one cell division (Fig. 6B–D). In some cases, multicellular filaments began developing immediately (Fig. 6I). Cells were variously shaped,

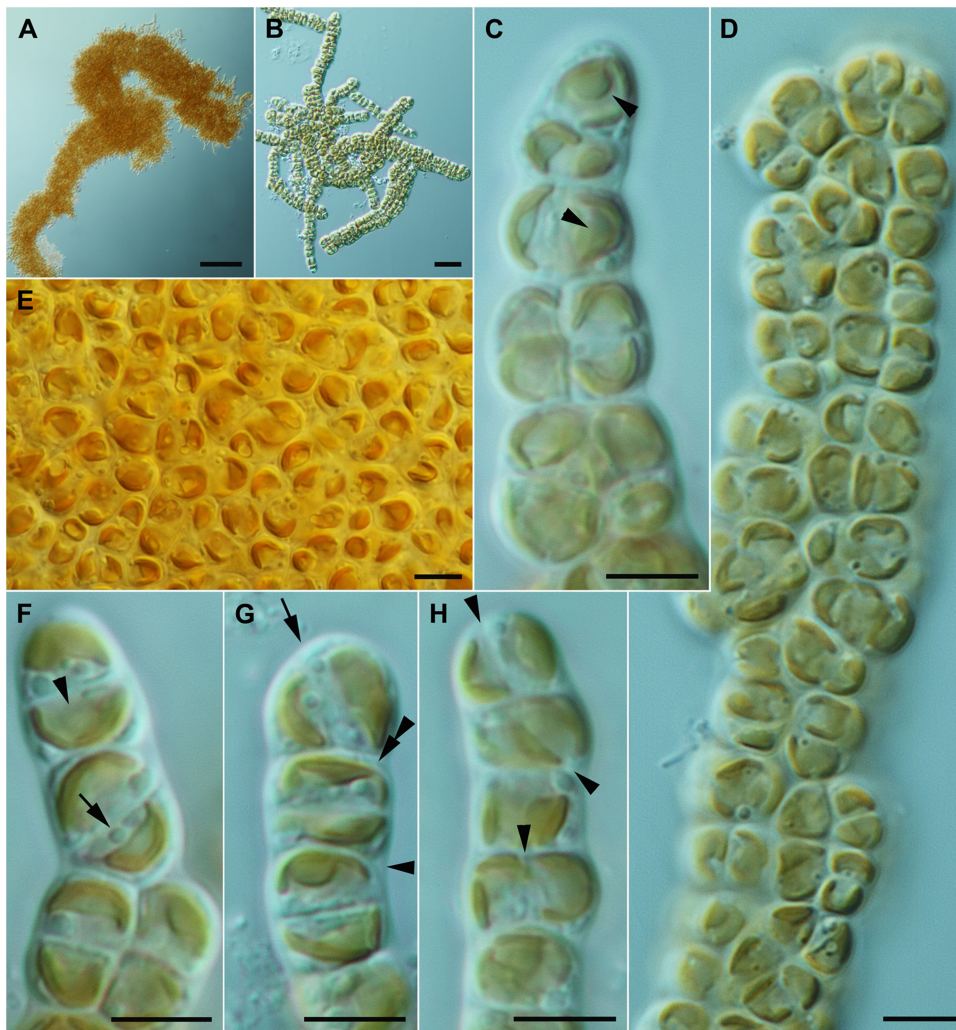


**Figure 4.** *Phaeosaccion multiseriatum* sp. nov. **A.** Thallus formed from basal cell mass and consisting of numerous uniseriate and multiseriate filaments. Scale bar = 100  $\mu\text{m}$ . **B.** Thallus of multiseriate branched filaments arising from a central area. Scale bar = 20  $\mu\text{m}$ . **C.** Filament tip showing early lateral division producing a multiseriate filament. Note the pyrenoid in the center of the chloroplast (arrowheads) Scale bar = 5  $\mu\text{m}$ . **D.** A solid multiseriate filament. Scale bar = 5  $\mu\text{m}$ . **E.** Thallus of parenchymatous-like cells with no obvious filamentous origin. Scale bar = 5  $\mu\text{m}$ . **F.** Filament tip showing cell divisions. Note the lipid droplet (arrow) and pyrenoid (arrowhead) Scale bar = 5  $\mu\text{m}$ . **G.** Uniseriate filament with apical cell dividing diagonally (arrow) and next two cells dividing more or less transversely. Note the cell walls (double arrowhead) and the mucilage sheath around the filament (single arrowhead). Scale bar = 5  $\mu\text{m}$ . **H.** Uniseriate filament showing diagonal or longitudinal cell division (arrowheads). Scale bar = 5  $\mu\text{m}$ .

some longer than wide, some cuboidal and some shorter than wide (Fig. 6). Cells were typically 4–7  $\mu\text{m}$  in size. Each cell was surrounded by a cell wall (Fig. 6H), and a thin mucilaginous sheath surrounded the filament (Fig. 6D, G, arrowheads). The walls and mucilaginous sheath were easily visible after staining with brilliant cresyl blue, ruthenium red, etc. (not shown). Cells had a single parietal chloroplast (Fig. 6F–I) except immediately before cell division (Fig. 6J, K, cell 2). The chloroplast

was usually slightly lobed, but on some occasions the plastid was deeply lobed (Fig. 6F, G). Some chloroplasts appeared to have a pyrenoid, but it was difficult to distinguish (Fig. 6G, I, arrow).

Zoospores were produced within 2 to 3 h after subculturing into new medium. The terminal cell of a filament divided, and the distal daughter cell became the zoospore (Fig. 6J, Supplementary Material Fig. S14). The distal daughter cell produced an eyespot during the division process. The



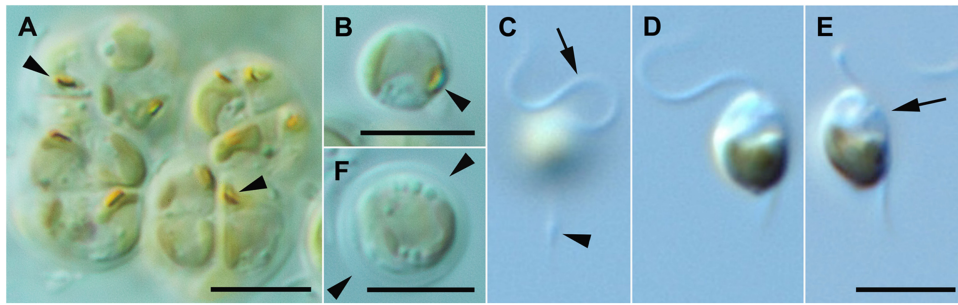


**Figure 5.** *Phaeosaccion multiseriatum* sp. nov. Scale bars = 5  $\mu\text{m}$ . **A.** Vegetative cells transforming to zoospores. Note the red eyespot (arrowheads). **B.** Pre-zoospore released after cell wall dissolved but before flagella developed. Note the eyespot (arrowhead). **C–E.** Three images of a zoospore; eyespot present but not visible. **C.** Long sinusoidal anterior flagellum (arrow) and short stiff posterior flagellum (arrowhead). **D.** Note the single posterior chloroplast. **E.** Note the insertion of the flagella (arrow). **F.** Zoospore after discarding flagella and extruding a basal mucilage pad (arrowheads). Eyespot was no longer present. (For interpretation of the references to color in this figure legend, the reader is referred to the web version of this article.)

zoospore was expelled, posterior end first, through a pore in the cell wall, or zoosporangium wall (Fig. 6J, Supplementary Material Fig. S14A–G). The flagella formed as the zoospore was leaving the zoosporangium, and the elongation of the flagella helped expel the zoospore from the zoosporangium (Supplementary Material Fig. S14G–L). The flagellar elongation process continued for about one to two minutes after release from the zoosporangium, and in the illustrated case, the posterior flagellum was attached to the coverslip (Supplementary Material Fig. S14L–P). In other cases, the zoospore agitated for one to two minutes as the flagella elongated (not shown). Once the flagella were fully formed, the zoospore swam away at a relatively high rate of speed. The zoosporangium wall seemed to contract once the zoospore was released, the pore was not clearly visible, and apparently the zoosporangium wall fused with the proximal daughter cell wall (Fig. 6K, Supplementary Material Fig. S14).

The zoospores were approximately  $3\ \mu\text{m} \times 5\ \mu\text{m}$  in size, with a pyriform shape (Fig. 6L, M, Supplementary Material Fig. S14M–S). The flagella were inserted approximately 1/3 the cell distance as measured from the anterior end. The chloroplast filled the posterior end of the zoospore and an eyespot was present (Fig. 6L, M, small arrow). The chloroplast often appeared cup-shaped, but it was actually a bilobed parietal chloroplast with the lobes cupped around the sides of the zoospore posterior end. In observed cases, the anterior flagellum attached to the substrate, the flagella were withdrawn into the cell, and the cell became quite flat against the substrate (Fig. 6N).

*Antarctosaccion applanatum* (Gain) Delépine. The specimen used for DNA extrac-

tion was collected as an epiphyte on *Plocamium cartilagineum* (Rhodophyta) from the infralittoral at around 10 m depth at Cheshire Island, a small islet at Rothera Point, Adelaide Island, Antarctica, on Dec. 31, 2010. Other collected specimens were dried on herbarium paper, and morphological examination showed that the specimens represented this species.

#### Tetrasporopsidaceae.

*Tetrasporopsis fuscescens* strain SAG 20.88. *Tetrasporopsis fuscescens* strain SAG 20.88 was not thoroughly examined using light microscopy. Zoospores were observed on one occasion but detailed observations could not be made. The zoospores resembled those formed by the Phaeophyceae, Phaeosacciophyceae, Phaeothamniophyceae and Xanthophyceae, i.e. laterally inserted flagella with longer anterior flagellum and shorter posterior flagellum (results not shown).

#### *Tetrasporopsis moei* sp. nov.

*Tetrasporopsis moei* produced semisolid irregular shaped colonies with occasional open areas (Fig. 7A, arrows). Large colonies were hard and some effort was needed to crush the colonies so that individual cells could be observed. Colonies attached to small plant roots in biphasic soil-water cultures and to cotton fibers that were added to cultures (Fig. 7B). Individual cells were spherical, surrounded by a cell wall and were usually 7–10  $\mu\text{m}$  in diameter (Fig. 7C, D), although cells from 5 to 15  $\mu\text{m}$  were occasionally observed (not shown). Each cell had one or two plate-like parietal chloroplasts and no pyrenoid was observed (Fig. 7C, D). The central cell region between the chloroplast lobes often contained refringent vesicles that were

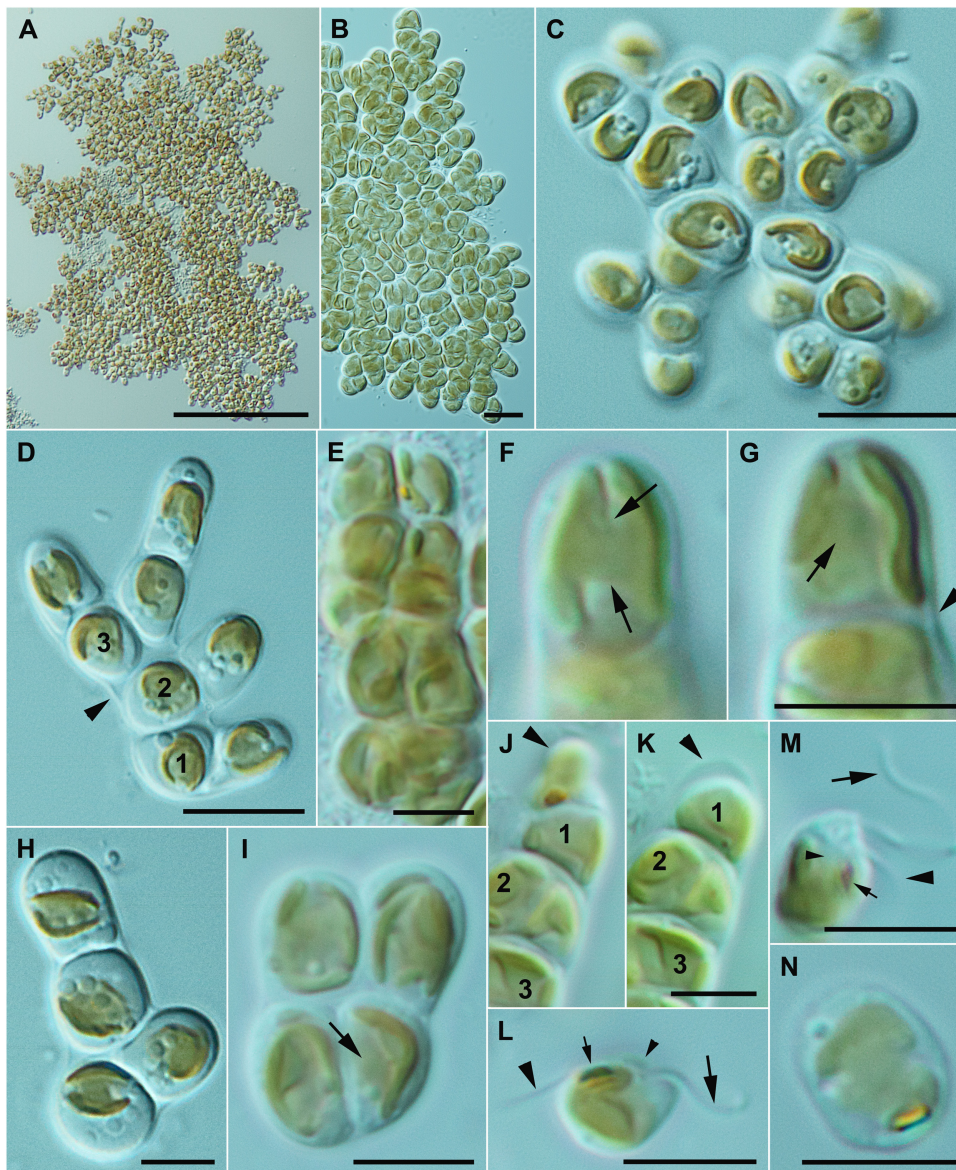


**Figure 6.** *Phaeosaccion okellyi* sp. nov. **A.** Large thallus-like structure formed by numerous short branches. Scale bar = 100  $\mu\text{m}$ . **B.** Thallus-like layer showing uniseriate and multiseriate filaments that were highly branched. Scale bar = 10  $\mu\text{m}$ . **C.** Thallus-like cluster of cells formed by very frequent branching. Scale bar = 10  $\mu\text{m}$ . **D.** Early stage of thallus development. Note the branch cells extended from the first, second and third cells of the filament. Note the mucilage sheath around the filament (arrowhead). Scale bar = 10  $\mu\text{m}$ . **E.** Multiseriate filament with some cells in clusters of four. Note the eyespot on one of the terminal cells. Scale bar = 5  $\mu\text{m}$ . **F, G.** Scale bar = 5  $\mu\text{m}$ . **F.** Cell showing the narrow isthmus connecting the two parietal chloroplast lobes (arrows). **G.** Same cell as F, showing the trough-like parietal plastid and a possible pyrenoid (arrow). Note the mucilaginous sheath (arrowhead). **H.** A filament from an older culture showing lipid droplets and chryso-laminaran. The single chloroplast was more centrally located. Scale bar = 5  $\mu\text{m}$ . **I.** Multiseriate filament forming from the initial two daughter cells. Note the pyrenoid-like structure. Scale bar = 5  $\mu\text{m}$ . **J, K.** Scale bar = 5  $\mu\text{m}$ . **J.** The beginning of zoospore release (arrowhead) from the zoosporangium captured on video (see Fig. S14). Filament cells 1–3 were labeled. Note that cell 2 was dividing and had two chloroplasts. **K.** The zoosporangium wall (arrowhead) was shown after the zoospore was released. Filament cells are numbered as in J. **L.** Zoospore showing the long anterior flagellum (large arrow), the short, stiff posterior flagellum (arrowhead) and the eyespot (small arrow) in the chloroplast. Note the flagellar insertion along the side of the zoospore (small arrowhead). Scale bar = 5  $\mu\text{m}$ . **M.** Zoospore showing the long anterior flagellum (large arrow), posterior flagellum (arrowhead) and eyespot (small arrow). Note the flagellar insertion (small arrowhead). Scale bar = 5  $\mu\text{m}$ . **N.** A very flattened cell formed after the zoospore attached and withdrew the flagella. The eyespot is still evident. Scale bar = 5  $\mu\text{m}$ .



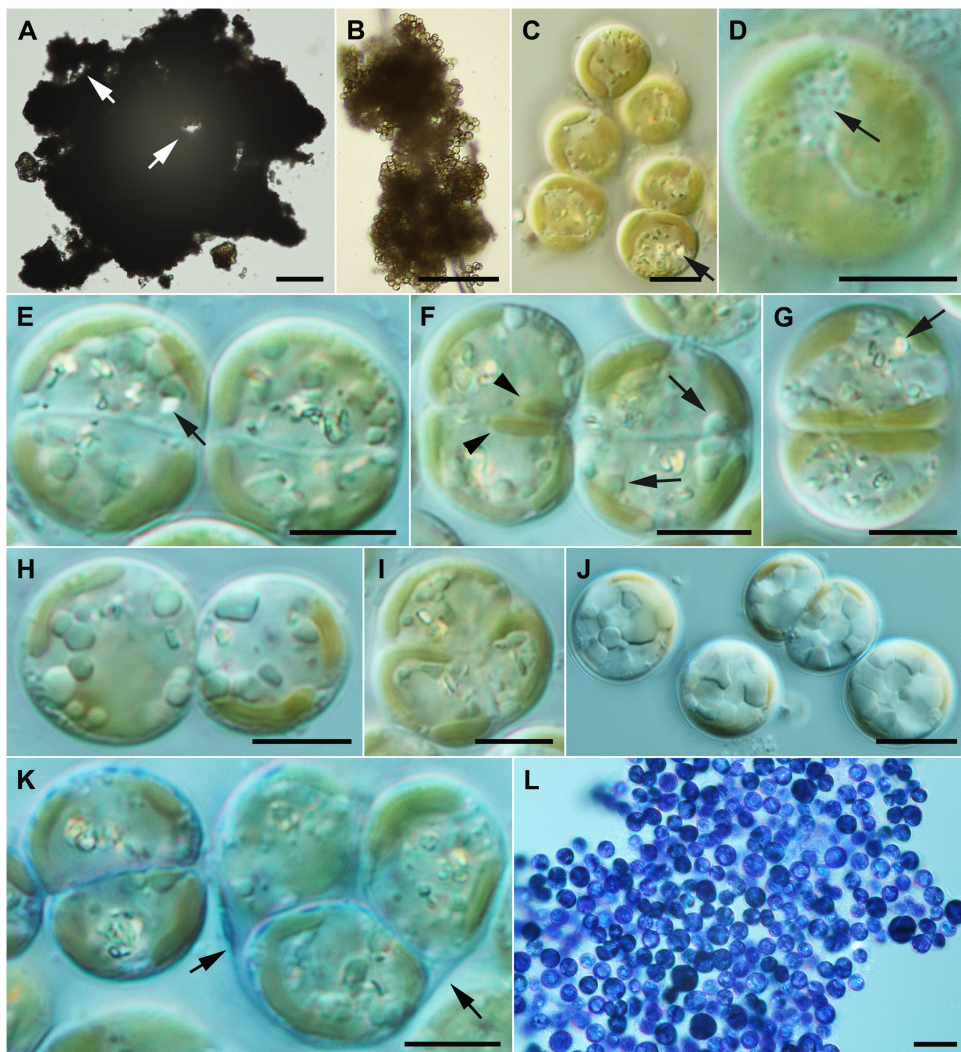


**Figure 7.** *Tetrasporopsis moei* sp. nov. **A.** Thallus showing solid (not hollow) cell mass with a few perforations (arrows). Scale bar = 100 μm. **B.** Young thallus forming around a cotton fiber. Scale bar = 100 μm. **C.** Vegetative cells showing the chloroplasts and "dancing particles" (arrow). Scale bar = 5 μm. **D.** Cell periphery showing the chloroplast lobes and peripheral vesicles (arrow). Scale bar = 5 μm. **E.** Two dividing cells showing the formation of the new cell walls between the daughter cells. Note the hemispherical shape of the daughter cells and the absence of chloroplasts along the forming walls. "Dancing particles" are present (arrow). Scale bar = 5 μm. **F.** Two dividing cells. The left cell has chloroplast lobes rotating along the forming cell walls (arrowheads). Note the lipid bodies in the right cell (arrows). Scale bar = 5 μm. **G.** Dividing cell with plastids along the forming cell walls. Note the "dancing particle" (arrow). Scale bar = 5 μm. **H.** Spherical daughter cells. Note the single bilobed chloroplast in each daughter cell. Scale bar = 5 μm. **I.** Tetrad formation with three daughter cells visible. Scale bar = 5 μm. **J.** Stationary phase cells with angular storage bodies. Scale bar = 5 μm. **K.** Dividing pair of cells (left) and tetrad of cells (right) lightly stained with brilliant cresyl blue. Note the gelatinous sheath around the tetrad of cells (arrows). Scale bar = 5 μm. **L.** Smashed thallus heavily stained with brilliant cresyl blue. Note the complete absence of gelatinous stalks. Scale bar = 20 μm.

actively moving ("dancing") via Brownian motion (Fig. 7C, G, arrows). Rapidly growing cells had a few peripheral vesicles (Fig. 7D, arrow) or lipid droplets (Fig. 6F, arrows). Rarely, a hematochrome body was observed (not shown). Vegetative cell

division occurred in two ways. Often, one cell would divide into two hemispherical daughter cells (Fig. 7E-G), and then the daughter cells became round as they grew (Fig. 7H). On occasion, a tetrad of daughter cells was formed (Fig. 7I, K). The four

660  
661  
662  
663  
664

cells eventually became spherical and separated as four independent cells (not shown). Cells from stationary phase cultures were packed with storage products that had an angular appearance (Fig. 7J). Cell walls stained with brilliant cresyl blue (Fig. 7K, L). With light staining, thin and thick wall areas were observed (Fig. 7K), and for tetrads, remnants of the mother wall were evident after being stained (Fig. 7K). Heavy staining with brilliant cresyl blue (Fig. 7L), ruthenium red, Lugol's iodine solution and methylene blue (not shown) failed to show any evidence of gelatinous stalks. Contractile vacuoles and swimming cells were not observed.

*Psammochrysis cassiotisii* gen. & sp. nov. strain EC38. The rounded, flattened unicells of *Psammochrysis cassiotisii* appeared as gold coins strongly adhered to sand grains collected from a high intertidal pool in Narooma Inlet, New South Wales, Australia and were 10–16  $\mu\text{m}$  in diameter including a cell wall (Fig. 8A, B). In enrichment cultures, benthic cells produced zoospores which were easily isolated into clonal culture from which the species was studied. In culture, the benthic stage dominated over a 24-h cycle, with zoospores only sparingly observed in a 2-h window after the lights came on. Zoospores settle near one another, in rafts, where they immediately divide, the daughter cells adhering adjacent to one another in pairs (Fig. 8A–D). As these cells mature and release zoospores, the pairs of parental cell walls remain (Fig. 8C, D). Zoospores typically settle and divide at the edge of rafts, and don't settle in space occupied by discarded parental walls towards the raft center (Fig. 8C, D).

Benthic cells have a central nucleus plus two, deeply-lobed chloroplasts each of the 4 lobes with a pyrenoid (Fig. 8A, B, J). The chloroplasts covered most of the cell surface and one lobe contained a small eyespot, most visible in zoospores (Fig. 8F–H). Each benthic cell enlarges and develops into a single, motile zoospore of the *Sarcinochrysis*-type, approximately twice the length (16–22  $\mu\text{m}$ ) of benthic daughter cells (Fig. 8E). The two heterokont flagella emerged subapically from a depression about a third of the way down the ventral surface (Fig. 8F, G). The long flagellum projected forward during motility, possessed tripartite hairs and was approximately the same length as the zoospore, while the short, trailing flagellum was smooth and approximately 2/3 the length of the zoospore. The lobes of both chloroplasts were concentrated at the apical end of the cell resulting in the opaque appearance of the posterior (Fig. 8E–G). A single eyespot is located within a lobe of the posterior chloroplast adjacent to the

site of flagella insertion (Fig. 8F–H). Zoospores were motile for a short period (i.e., 10–15 mins at most) before hovering above the substratum, weakly attached to it with their flagella. Zoospores began to round-up and flatten (Fig. 8H–J), cell division commenced immediately and daughter cells subsequently adhered strongly to the substratum (Fig. 8K, L).

### Chrysoaparadoxophyceae

*Nematochrysis sessilis* var. *vectensis*. Filaments were uniseriate in cultures less than two weeks old (Fig. 9A, B). Filaments grown on flooded L1 agar plates became quite long, at least up to 2–3 mm in length (Supplementary Material Fig. S15A, B). Filaments were from 2–8  $\mu\text{m}$  wide. Uniseriate filaments formed because adjacent cell walls were connected and because a thin gelatinous sheath surrounded the cells, although this was only evident after staining with ruthenium red (Fig. 9C, arrow, arrowheads) or other stains (brilliant cresyl blue, methylene blue; not shown). As cultures aged, occasional cells divided laterally (Fig. 9D, arrows), and as this lateral growth continued, the filament became somewhat brush-like as the lateral cells grew outward (Fig. 9E). Cell division became irregular and the organism changed from a filament to a palmelloid mass (Fig. 9F). Aplanospore-like structures developed in older cultures. Initially, the cells divided once or twice to produce stacked cells that apparently lacked cell walls (Fig. 9G, arrows), and with additional cell divisions, several cells formed inside the original mother cell wall (Fig. 9H, Supplementary Material Fig. S15D). Although not fully documented, it appeared that the mother wall dissolved and the aplanospore-like cells were released to give rise to new uniseriate filaments. In extremely old cultures (>2–3 months), uniseriate filaments with thick mucilaginous walls were observed (Supplementary Material Fig. S15E).

Block-like cells were 2 to 6  $\mu\text{m}$  in size, often square, sometimes shorter than wide, sometimes longer than wide (Fig. 9, Supplementary Material Fig. S15). In older cultures, some cells became as much as 10  $\mu\text{m}$  (Supplementary Material Fig. S15E). Typical vegetative cells had one or two parietal chloroplasts; in some cases, the isthmus between chloroplast lobes was apparent and in other cases it appeared as though two chloroplasts were present (Fig. 9A). A pyrenoid was sometimes observed in the plastid (Fig. 9B, right filament, arrowheads). Cells typically had few inclusions, but some cells had a lipid body (Fig. 9B, right fila-



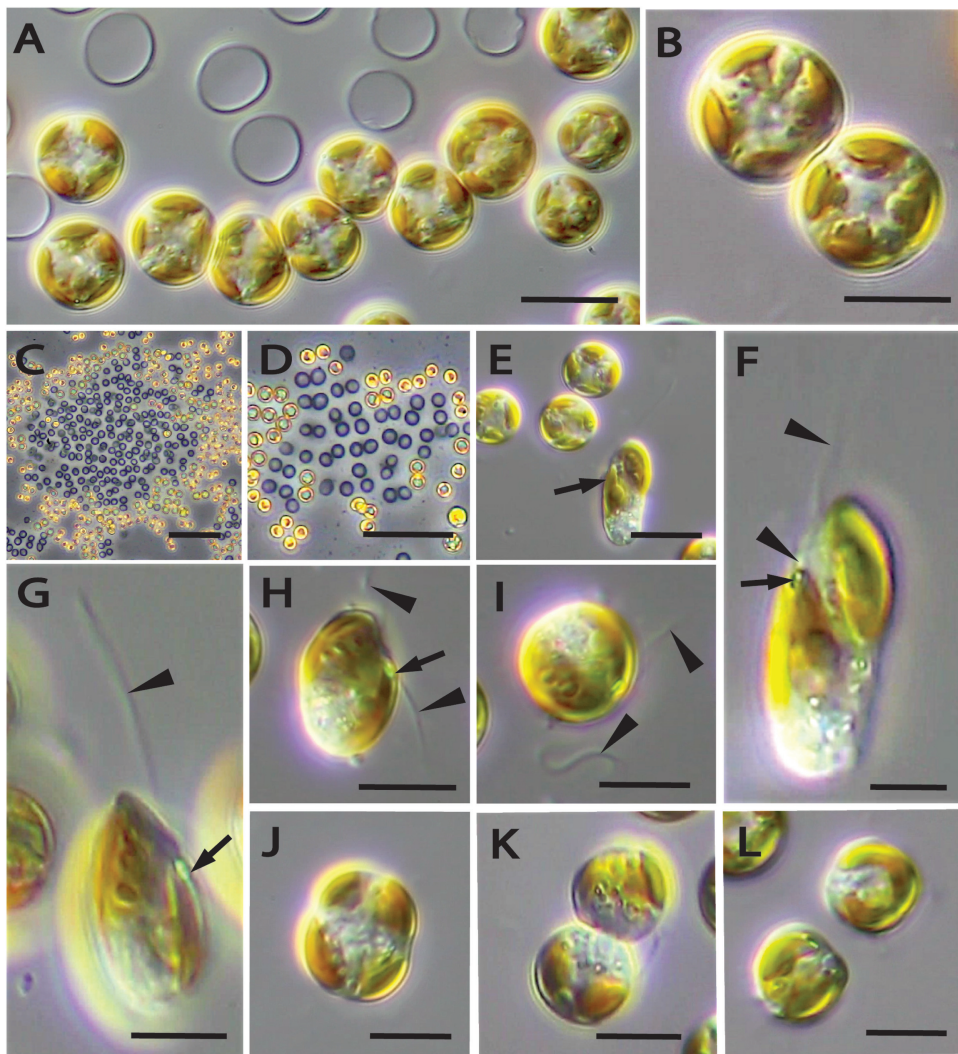


**Figure 8.** *Psammochrysis cassiotisii*. **A.** Benthic cells and remnant cell walls at the edge of a raft (see rafts in C and D). Scale bar = 20  $\mu\text{m}$ . **B.** Higher magnification of a pair of mature cells (i.e., daughter cells). Cells flat and rounded with 2, deeply lobed chloroplasts. Scale bar = 10  $\mu\text{m}$ . **C.** Raft structure with benthic cells on the rim, remnant cell walls in the interior. Scale bar = 100  $\mu\text{m}$ . **D.** Small raft, benthic cells and empty cell walls following zoospore escape are in pairs. Scale bars = 70  $\mu\text{m}$ . **E.** Zoospore (arrow) are elongate compared to the benthic cells that develop into them. Scale bar = 15  $\mu\text{m}$ . **F.** Zoospore with long flagellum (arrowheads) originating from a subapical depression on the ventral surface. A small eyespot (arrow) is in a lobe of the posterior chloroplast near the point of flagella insertion. Cell posterior is opaque and does not contain either chloroplast. Scale bar = 5  $\mu\text{m}$ . **G.** Same cell as in figure F, different orientation, showing the long flagellum (arrowhead) and eyespot (arrow). Scale bar = 5  $\mu\text{m}$ . **H.** Zoospore rounding up and preparing for division, hovers above the surface of the coverslip attached by its two flagella (arrowheads) that are largely out of the plane of focus. Eyespot (arrow). Scale bar = 10  $\mu\text{m}$ . **I.** Rounded zoospore preparing to divide, attached to the coverslip by the flagella (arrowheads) that are largely out of the plane of focus. Scale bar = 10  $\mu\text{m}$ . **J.** Settled zoospore hovering about the coverslip surface, rounded-up at the beginning of cell division. Scale bar = 10  $\mu\text{m}$ . **K.** Cell division of zoospore observed in figures H - J. Each daughter cell has a single, 2 lobed chloroplast. Scale bar = 10  $\mu\text{m}$ . **L.** Following division, daughter cells adhere tightly to the coverslip surface. Scale bar = 10  $\mu\text{m}$ .

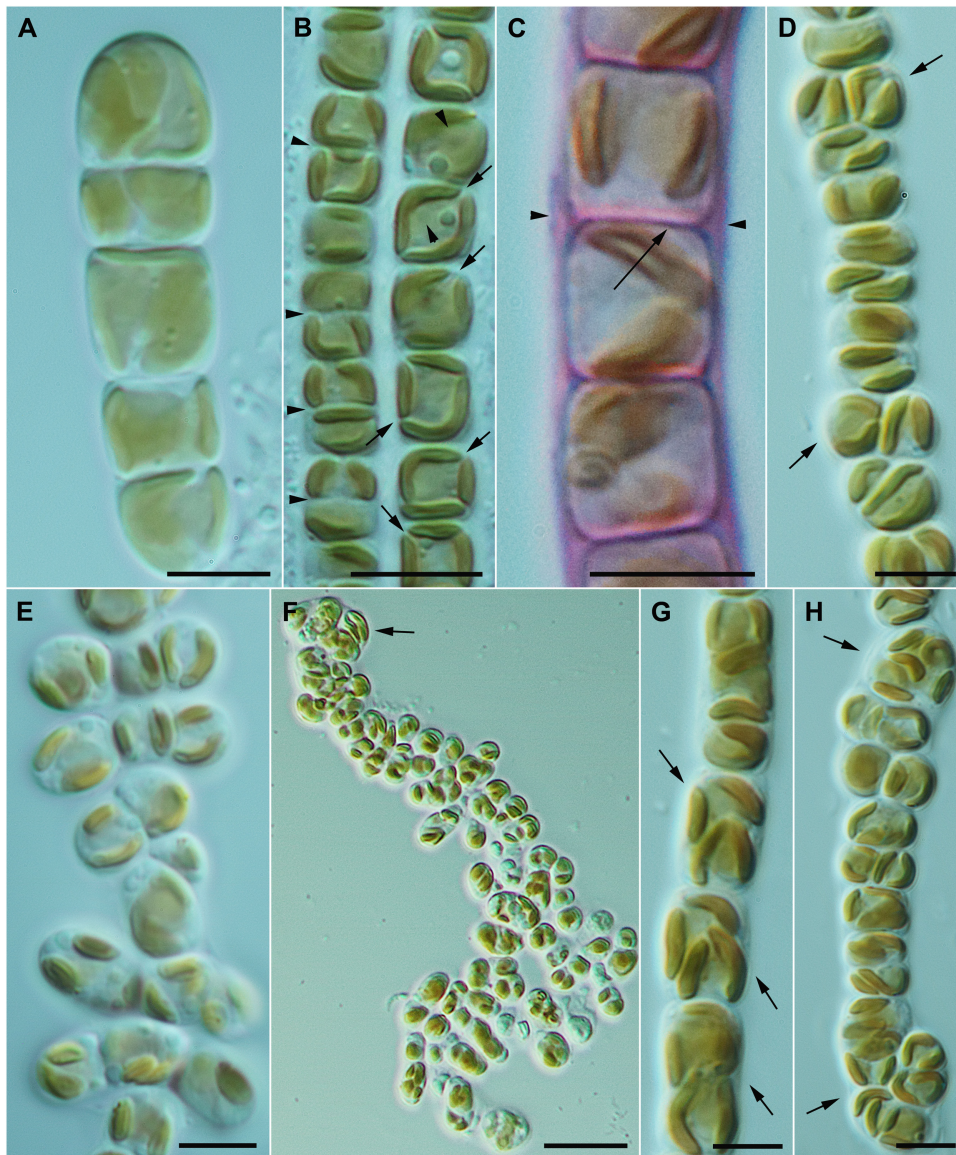


**Figure 9.** *Nematochrysis sessilis* var. *vectensis*. **A.** Short filament with 1 deeply bilobed chloroplast or two chloroplasts. Scale bar = 5  $\mu\text{m}$ . **B.** Two parallel filaments. Left filament shows daughter with transverse cell division (arrowheads). Right filament showing pre-cell division with diagonal chloroplast division (arrows). Note the pyrenoid-like structures on the left filament (arrowheads). Scale bar = 5  $\mu\text{m}$ . **C.** Fused cell walls (arrow) and a filament sheath (arrowheads) stained with ruthenium red. Scale bar = 5  $\mu\text{m}$ . **D.** Lateral cell division (arrows) in an early stage of multiserial filament formation. Scale bar = 5  $\mu\text{m}$ . **E.** Early stage of palmella formation where the multiserial filament has a brush-like appearance. Scale bar = 5  $\mu\text{m}$ . **F.** Palmella stage with irregularly organized cells. Note also the aplanospore sporangium (arrow). Scale bar = 20  $\mu\text{m}$ . **G.** Early stage of aplanospore formation with two cells per future sporangium (arrows). Scale bar = 5  $\mu\text{m}$ . **H.** More advanced stage of aplanospore sporangium development with several cells inside the sporangia (arrows). Scale bar = 5  $\mu\text{m}$ . (For interpretation of the references to color in this figure legend, the reader is referred to the web version of this article.)

ment), and peripheral vesicles were observed after staining with brilliant cresyl blue (Supplementary Material Fig. S15C). Prior to cell division, the chloroplast divided diagonally to produce two chloroplasts (Fig. 9B right filament, arrows). Even though chloro-

plast division was diagonal, by the time cytokinesis was completed, the protoplasts had rotated so that the new cell walls were transverse (Fig. 9B, left filament, arrowheads).

773  
774  
775  
776  
777  
778  
779  
780  
781



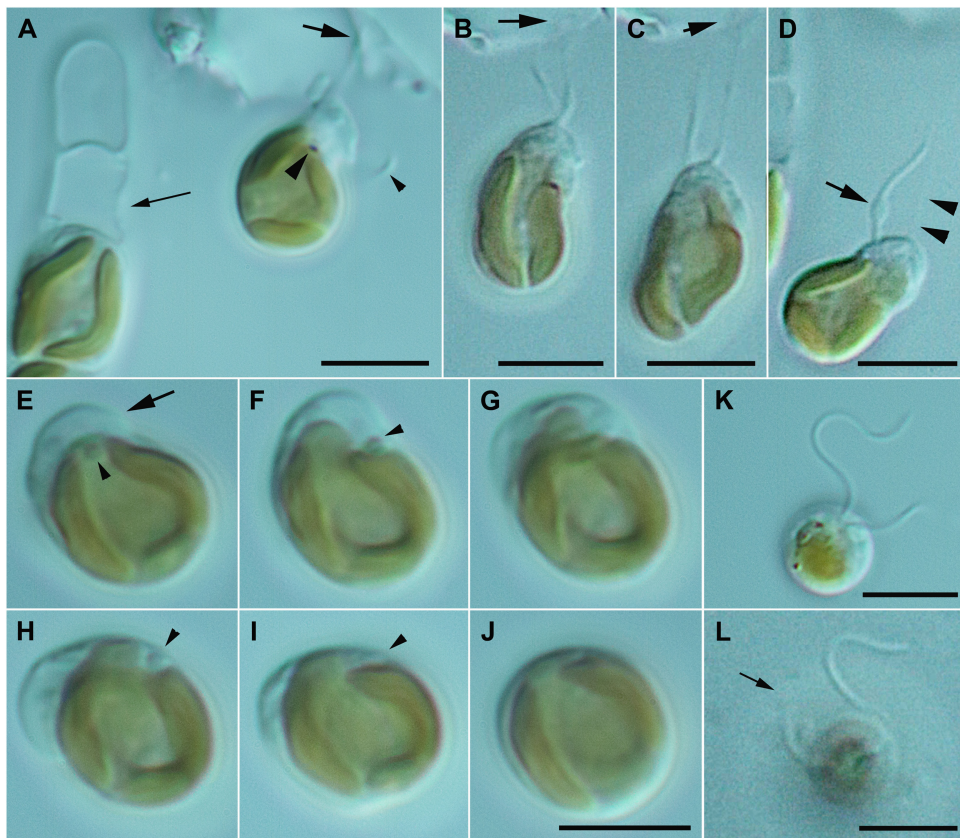


**Figure 10.** *Nematochrysis sessilis* var. *vectensis*. **A–J.** Observations of zoospore release, attachment and transformation to a vegetative cell. Scale bars = 5  $\mu$ m. **A.** Biflagellate zoospore that recently escaped through a cell wall pore (small arrow). The long flagellum (large arrow) was attached to a fragment of glass, the short flagellum (small arrowhead) was beating slowly, and the eyespot (large arrowhead) is visible. Note the lobe-like cytoplasmic extension. **B, C, D.** Three images captured from a video sequence showing a movement away from the fragment (arrows in B, C) as the long flagellum becomes thinner and longer (arrowheads). The short flagellum produced a swelling (arrow) and was retracted. **E–J.** Zoospore has retracted the flagella and attached to the microscope slide. The cytoplasmic extension changes position as the cell rounds up and transforms to a vegetative cell. **K.** Spherical zoospore appearing like an *Ochromonas*-type cell. Note that the posterior flagellum is not over the eyespot. **L.** Spherical zoospore attached at the tip of the posterior flagellum (arrow). Note the nearly 180-degree orientation of the flagella at the point of insertion. From video.

782 The onset of zoospore formation was signaled  
 783 by the presence of an eyespot on chloroplasts  
 784 of slightly swollen vegetative cells ([Supplementary](#)  
 785 [Material Fig. S15F](#)). A single zoospore was formed  
 786 and the zoospore escaped, posterior end first,  
 787 through a pore in the cell wall ([Fig. 10A](#)). Zoospores  
 788 were approximately 5 by 7  $\mu$ m in size. Zoospores  
 789 had a single chloroplast, but at times the plas-  
 790 tid lobes appeared like two separate chloroplasts  
 791 ([Fig. 10B, C](#)). Zoospores were biflagellate, with a  
 792 long anteriorly directed flagellum that beat with a  
 793 sinusoidal wave and with a short stiff posterior fla-  
 794 gellum. An eyespot was present at first ([Fig. 10A–C](#))  
 795 but was gradually lost ([Fig. 10D, E](#)). One zoospore  
 796 was captured in a video and on still images after it

797 escaped from the vegetative cell (zoosporangium)  
 798 and immediately attached with the anterior flagel-  
 799 lum to a fragment of glass ([Fig. 10A](#)). Initially, it  
 800 appeared like the zoospore was going to settle on  
 801 the glass fragment, but then the anterior flagellum  
 802 elongated and became thin, pushing the cell away  
 803 from the fragment ([Fig. 10B, C](#)). The short flagel-  
 804 lum enlarged before it was withdrawn ([Fig. 10D](#)),  
 805 and the two flagella were no longer visible. The  
 806 cell showed a slight amoeboid movement as it  
 807 became round and attached to the microscope cov-  
 808 erslip ([Fig. 10E–J](#)). Throughout the entire process,  
 809 the anterior end of the zoospore exhibited amoeb-  
 810 oid movement as it transformed from a zoospore  
 811 to an attached vegetative cell. In other cases,

zoospores swam for a while and became spherical in shape (Fig. 10K, L). At times, the spherical cells looked exactly like an *Ochromonas*-type cells, but notice that the short flagellum is not associated with the eyespot (Fig. 10K). Spherical cells were observed attaching to the substrate by the posterior flagellum, and they spun around for about one to two minutes before the flagella were retracted and the cells flattened as shown (Fig. 10E–J). Finally, aplanospore-like structures were observed (Supplementary Material Fig. S15D), but these were rare and could not be fully described.

## Discussion

### Phaeosacciophyceae classis nov.

The classification of *Phaeosaccion*, *Tetrasporopsis*, *Nematochrysis*, *Chrysomeris* and “*Giraudyopsis*” has been controversial. Farlow (1882) described *Phaeosaccion collinsii* as a simple or primitive brown alga. *Tetrasporopsis* was first described as *Tetraspora fuscescens* (Braun in Kützing 1849), transferred to *Phaeocystis* in the new generic section *Tetrasporopsis* (De Toni 1895), and then it was raised to generic level and classified in the Phaeophyceae (Lemmermann 1899). *Nematochrysis* and *Chrysomeris* were classified in the Chrysophyceae (Bourrelly 1957; Carter 1937; Pascher 1914a,b, 1925; Schussnig 1940; Waern 1952). Finally, Dangeard (1965, 1966) described “*Giraudyopsis*” as a simple brown alga. All of these genera have been reclassified in the past 50 years. As one example, *Phaeosaccion collinsii* was re-classified in the Chrysophyceae (Chen et al. 1974), Phaeothamniophyceae (Cryan et al. 2015; Mathieson and Dawes 2017) and Chrysomeridophyceae (Gabrielson and Lindstrom 2018).

One genus, *Chrysomeris*, has not been examined using molecular phylogenetic analysis, its classification remains uncertain, and this has caused many problems. Carter (1937) described *Chrysomeris* with two species, each forming uniflagellate zoospores, and Bourrelly (1957) designated *C. ramosa* as the type species. Schussnig (1940) described *C. simplex* Schussnig but did not observe zoospores. Gayral and Haas (1969) described an alga using the name *C. ramosa* but with very different characteristics (see Table 1). Briefly, Carter (1937) described *C. ramosa* with a pyriform zoospore with one flagellum and no eyespot. Gayral and Haas (1969) described an oval zoospore with two flagella and a large eyespot. Gayral and Haas (1969) stated that the second flagellum was 10  $\mu\text{m}$  long, and they suggested that

Carter (1937) had failed to observe the second flagellum. Given the other uniflagellate and biflagellate cells that were described with impeccable accuracy by Carter (1937), it doesn't seem likely that she overlooked a 10  $\mu\text{m}$  second flagellum. Carter described a zoosporangium where numerous naked zoospores were formed in the gelatinous sheath, and the zoospores were released via breaks or dissolution of the sheath. Gayral and Haas (1969) described zoospore formation where a single zoospore was formed from a vegetative cell and escaped through a pore in the cell wall. Carter (1937) described vegetative cells with three plastids, rarely two and more rarely one. Conversely, Gayral and Haas (1969) described vegetative cells with one plastid or rarely two in old cells. Additional differences are listed in Table 1. In summary, Gayral and Haas (1969) studied an alga that was misidentified as *C. ramosa*.

The situation was further complicated by the descriptions of order and class names that were not based on Carter's (1937) protologue but rather on the misidentified alga studied by Gayral and Haas (1969). Specifically, Cavalier-Smith (in Cavalier-Smith et al. 1995) described the class Chrysomerophyceae cl. nov. T. Cavalier-Smith, 1995 nom. typificatum (type *Chrysomeris*). The correct Latin spelling is Chrysomeridophyceae, not Chrysomerophyceae; the misspelling is correctable (see Art. 61.4 of the ICN, Turland et al. 2018). Despite the diagnosis (see Cavalier-Smith et al. 1995), the name was explicitly formed from a generic name, it is an automatically typified name and must be applied to a class that includes the type of *Chrysomeris ramosa* N. Carter (see Art. 16.1 & 16.2, Art 10.10, Turland et al. 2018).

Uniflagellate cells or uniflagellate zoospores are known for the Chrysophyceae (including Synurophyceae), Coscinodiscophyceae, Dictyochophyceae, Eustigmatophyceae, Mediophyceae and Pelagophyceae, and both uniflagellate and biflagellate swimming cells are known for the Chrysophyceae, Dictyochophyceae, Eustigmatophyceae and Pelagophyceae. Conversely, all swimming cells are biflagellate for classes belonging to the SI clade of the heterokont algae. As such, it seems unlikely that *Chrysomeris ramosa* N. Carter and the Chrysomeridophyceae belong within the SI clade. Therefore, the new class Phaeosacciophyceae is proposed for *Antarcosaccion*, *Phaeosaccion*, *Psammochrysis* and *Tetrasporopsis*.

**Table 1.** Morphological comparisons of *Chrysomeris ramosa* N.Carter (1937) and the alga observed by Gayral and Haas (1969).

Character	N. Carter	Gayral & Haas
<b>Zoospores</b>		
No. flagella on zoospore	1	2
Flagellum length, anterior	1 × cell length	1 ×–1.5 × cell length
Flagellum length, posterior	N.A.	10 μm
<b>Zoospore shape</b>		
Zoospore size	17 μm × 10 μm	Oval
Zoospore plastid no.	Three or two (band-shaped)	10–15 μm × 6–8 μm
Zoospore eyespot	Absent	One or two (trough-like) present (large)
Zoospore formation	Many zoospores formed without cell walls directly into enlarged filament sheath	One zoospore formed per cell, cell wall retained.
Zoospore release	Filament sheath tears/dissolves to release several or all zoospores	Individual pore formed in each cell wall to release a single zoospore
<b>Filamentous cells</b>		
Uni- and multiseriate	Yes	Yes
Filament diameter	8–35 μm	est. 10–30 μm
Cell diameter	8–12 μm	est. 7–15 μm
Number plastids	3 (rarely 2, more rarely 1)	1, rarely 2 in old cells
Cytoplasmic rods (1 μm)	Absent	Present
Muciferous bodies	Absent	Present
Chrysolaminaran	Absent	Present
Globules (fat)	Present	Present
Substrate	On <i>Spartina</i>	On <i>Bostrychia</i>
Basal cell	Mostly like vegetative cells	Very different from veg. cells
Aplanospores	Absent	Present
Boutures	Absent	Present
Pseudocysts	Absent	Present

### Phaeosaccion and Antarctosaccion

We have shown with gene sequences that *Phaeosaccion collinsii* does not belong in the Chrysophyceae, Phaeophyceae or Phaeothamniophyceae. We examined two strains that were identified in culture collections as “*Giraudyopsis*”, but we found they were closely related to *Phaeosaccion collinsii*. Furthermore, Wynne and Furani (2014) showed that “*Giraudyopsis stellifer*” (Dangeard 1965) was not validly published because no type specimen was designated (Art. 40.1, Turland et al. 2018). Similarly, “*Giraudyopsis stelliger* var. *typica*” and “*G. stelliger* var. *condensata*” were not validly published (Dangeard 1966). [For an unknown reason, Dangeard changed the intended epithet from “*stellifer*” to “*stelliger*” in the second paper.] There are substantial morphological differences between *P. collinsii* and the two new species *P. multiseriatum* and *P. okellyi*, but nevertheless, all three species produce uniseriate and multiseriate filaments (Figs 3, 4, 6, McLachlan

et al. 1971). *Antarctosaccion* and *Phaeosaccion* are sister taxa, and we consider the branch lengths significantly long enough to warrant generic separation. Interestingly, *Antarctosaccion applanatum* and *Phaeosaccion collinsii* are morphologically similar but genetically distinct. It remains unclear if “*Giraudyopsis*” sensu Dangeard (1965) and the alga studied by Gayral and Haas (1969) are related to *Phaeosaccion* or are related to algae in some other class (e.g. Pelagophyceae). On the other hand, based on the 18S rRNA sequence identity, it appeared that the alga reported from New Zealand by Broom et al. (1999) corresponds to our *P. multiseriatum*.

### Tetrasporopsis

Using a portion of the *Tetrasporopsis fuscescens* lectotype, we showed that the type material was genetically close to culture strain SAG 20.88. Strain SAG 20.88 was isolated in 1975 from a pond near Arazedo, Portugal has been used to rep-



resent the genus in molecular phylogenies (e.g. Yang et al. 2012). Therefore, the phylogenetic position of this strain in molecular phylogenies can be regarded as representative of the lectotype for *Tetrasporopsis fuscescens*. Recently, *T. fuscescens* was reported from California (USA) and its gross colony morphology and cell structure strongly resembled *T. fuscescens*; however, the cells sat on gelatinous stalks that were visible after staining (Stancheva et al. 2019). Molecular phylogenetic analysis showed that the lectotype material, SAG 20.88 and the California organism all belonged to the same species.

Gene sequences place *T. fuscescens* and *T. moei* as sister taxa. Staining of the *T. moei* colonies show no gelatinous stalks. Morphologically, *T. moei* grows as a solid, irregular cluster of cells that is somewhat perforate. Two species with perforate colonies were classified in *Tetrasporopsis* by Starmach (1985), but they were transferred to *Dermatochrysis* (Entwistle and Andersen 1990). *Phaeosphaera gelatinosa* West & West resembles *T. moei* in having a perforate colony, but *P. gelatinosa* lacks cell walls and cell sizes are 14–17.5  $\mu\text{m}$ , nearly twice as large as for *T. moei* (West and West 1903).

### Psammochrysis

This unicellular species is sand-dwelling with a benthic stage that secretes a thick, adhesive wall in order to maintain its position in a dynamic, tide pool habitat. In most sand-dwelling algae, cell division occurs only in the benthic stage, where cells are tightly attached to the substrata. In the case of *P. cassiotisii*, benthic cells do not divide, but rather enlarge and differentiate into single zoospores that are released from the parental wall that is left behind. Zoospores are short lived and initially adhere only by the tips of their flagella. This weak adhesion maintains zoospores in position while they undergo cell division just off the substratum. Immediately following division, the daughter cells adhere strongly to the substratum adjacent to one another and synthesize thick, adhesive cell walls. During division, dividing cells can be easily removed from the coverslip by a gentle movement of the culture flask, yet you could say they are dividing in an attached state (i.e. benthic). This division cycle is similar to *Chrysoparadoxa australica* (Wetherbee et al. 2019), where benthic cells produce a single zoospore that leaves a thick wall behind following release, but in this case the zoospore adheres strongly to the surface prior to dividing (Wetherbee et al. 2019). It

seems counter intuitive that *P. cassiotisii* would be so weakly attached to a surface, and susceptible to being washed away, at arguably the most important stage of the cell cycle. However, perhaps this species' overall distribution is improved by daughter cell dislodgement since zoospores are short-lived and tend to remain close to the parental raft after release.

The multi-gene phylogeny shows that *Psammochrysis* forms a lineage distinct from other sequenced Phaeosacciophyceae, with a relatively long branch lengths separating it from its sister lineage *Tetrasporopsis*. The combination of its distinctive placement in the phylogeny and the unique morphological traits it possesses indicates that it should be considered a separate genus from *Tetrasporopsis*.

### Chrysoparadoxophyceae

#### Nematochrysis

Our observations of *Nematochrysis sessilis* var. *vectensis* collected from the type locality agree, in most parts, with the organism described by Carter (1937). We interpreted the highly lobed chloroplast as normally a single chloroplast per cell (Fig. 9A) whereas Carter described two or three chloroplasts, which seem apparent in some of our images (e.g. Fig. 9E). In addition, we observed aplanospore-like structures (Fig. 9G, H, and Supplementary Material Fig. S15D) that were not reported by Carter.

The type species is *Nematochrysis sessilis* Pascher, which was found in a Prague tank that was filled with water collected from the Adriatic Sea (Trieste) (Pascher 1914a,b, 1925). The cells of this alga were approximately 10  $\mu\text{m}$   $\times$  15  $\mu\text{m}$  (see Pascher 1925 for correction of an earlier erroneous size measurement). This alga has not been reported again. Carter (1937) described *N. sessilis* var. *vectensis* from a pond in Bembridge, Isle of Wight, UK. The filaments were 2–5  $\mu\text{m}$  wide, with cells shorter than wide to 1.5 $\times$  as long as broad. This alga was not reported again until we re-isolated it from the type locality. *Nematochrysis pusilla* Schussnig (1940) was collected from the Adriatic Sea (former German-Italian Institute for Marine Biology in Rovigno, now located in Croatia), and water was transported back to his Vienna laboratory. Schussnig (1940) pointed out that while it looked similar to brown algal germlings, it had more chrysophyte characteristics. The cells were 6 to 6.5  $\mu\text{m}$  in size and filaments were up to 40  $\mu\text{m}$  long. No zoospores were observed. *Nematochrysis hieroglyphica* Waern was collected from the



Oregrund Archipelago, Uppsala, Sweden (Waern 1952). Filaments were up to several hundred micrometers in length, and cells were 4.5–4.8  $\mu\text{m}$  wide and 3–6  $\mu\text{m}$  long. All four of these taxa were attached to the substrate by a basal gel pad.

Gayral and Lepailleur (1971) collected an alga from the Orne Estuary, France, that they considered identical to *Nematochrysis hieroglyphica*. They found that zoospores had laterally inserted flagella. Interestingly, Carter (1937) and Waern (1952) illustrate zoospores that appear to have lateral insertions of the flagella; Schussnig (1940) did not observe zoospores. We included in this study an alga identified as *Nematochrysis hieroglyphica* (culture strain K-0368 = CCMP3280) that was collected by Aase Kristiansen from near Svino, Zealand, Denmark. Based upon morphological observations (not shown) and gene sequence analysis (Fig. 2), this alga is sister taxon to *Nematochrysis sessilis* var. *vectensis*.

Gayral and Lepailleur (1971) combined the name as *Chrysowaernella hieroglyphica* (Waern) Gayral & Lepailleur. They provided three arguments: (1) the existence of longitudinal divisions for *N. hieroglyphica* but not for *N. sessilis*; (2) oblique cell division and protoplast rotation in *N. sessilis* but not for *N. hieroglyphica*; and (3) an *Ochromonas*-like insertion of flagella for *N. sessilis* but a lateral insertion of flagella for *N. hieroglyphica*. These arguments are countered here: (1) Pascher illustrates and describes “longitudinal” cell division when *N. sessilis* forms the palmella stage (Pascher 1925, Plate 15, fig. 2). (2) Oblique cell division is implied by Waern’s illustration and description (1952, fig. 32d), and Waern specifically chose the epithet “hieroglyphica” because of the angular (diagonal) chloroplasts that resembled the Egyptian hieroglyphics. (3) Pascher described zoospore release as Carter (1937) and as we also do for *N. sessilis* var. *vectensis*. Our released zoospore, when attached to the glass fragment, gives the appearance of an *Ochromonas*-type flagellar insertion (Fig. 10A–D) and the spherical zoospores sometimes looked exactly like an *Ochromonas*-like cell (Fig. 10K); nevertheless, the flagella are inserted laterally (Fig. 10L). Furthermore, Pascher specifically described *N. sessilis* zoospores as like those of *Phaeothamnion*, and *Phaeothamnion* definitely has lateral insertion of the flagella (Andersen et al. 1998; Graf et al. 2020). Consequently, we do not accept the classification of Waern’s (1952) alga in the genus *Chrysowaernella*, and we used the original name *Nematochrysis hieroglyphica*.

Our strains of *C. sessilis* var. *vectensis* require ammonia, i.e. they will not grow using nitrate as a

nitrogen source. The occurrence of *Nematochrysis* in aquarium tanks (e.g. Pascher 1925; Schussnig 1940) and estuaries (Carter 1937; Gayral and Lepailleur 1971; Waern 1952) may suggest that the requirement for ammonia is common in the genus.

## Phylogeny

*Nematochrysis* was recovered as sister to *Chrysoparadoxa* in the five-gene phylogenetic analysis (Fig. 2); however, statistical support was weak and few morphological characters are shared between the two genera. Both genera attach to substrates and because *Chrysoparadoxa* grows on K medium, we assume both have a requirement for ammonia. Both genera share similarly shaped flagellate cells but this similarity is shared across all the SI clade. Conversely, *Chrysoparadoxa* has a chloroplast surrounded by only two membranes, and this differs from all known heterokonts (Wetherbee et al. 2019). Most studies of *Nematochrysis* have been based upon light microscopy and Billard’s (1984) TEM examination of *Nematochrysis hieroglyphica* (as *Chrysowaernella hieroglyphica*) is inconclusive, therefore we do not know the chloroplast membrane number for *Nematochrysis*. Nevertheless, there is doubt about the inclusion of *Nematochrysis* in the Chrysoparadoxophyceae. We suggest for now including the two genera in the same class so as to avoid creating another single genus class within the SI clade. Further study, such as phylogenomic analyses, will confirm or contradict our classification.

Our study focuses only on the SI clade (sensu Yang et al. 2012), and therefore we do not provide any further insights into the overall phylogeny of the photosynthetic heterokonts. A plastid genomic study, with relatively few heterokont taxa and an emphasis on alveolate plastids, more or less supports the SI, SII and SIII clades; however, the authors suggest the Pinguiphyceae may belong in the SIII clade, not the SII clade (Ševčíková et al. 2015). Similarly, a phylogenomic study generally recovers the SI, SII and SIII clades and states “.. agreed with previous multigene phylogenetic analyses (Riisberg et al. 2019; Ševčíková et al. 2015; Yang et al. 2012)” (Derelle et al. 2016). Nevertheless, the origin of the photosynthetic heterokonts and final phylogenetic relationships of clades and classes within the group remain elusive.

## Other taxa

We included *Phaeobotrys solitaria* Ettl (SAG 15.95) and *Pleurochloridella botrydiopsis* Pascher

(CCMP1665) in this study because we thought they might help resolve the branching in the area of the Phaeophyceae, Xanthophyceae and taxa studied here. These two taxa branched at the base of the Xanthophyceae (Fig. 2). *Pleurochloridella botrydiopsis* (not the type species) was classified in the Heterokontae (= Xanthophyceae) (Pascher 1939) but *Phaeobotrys solitaria* (type species) was classified in the Chrysophyceae (Ettl 1966). Both taxa require further investigations, which are beyond the scope of this study.

The invalid "*Giraudyopsis*" has been thoroughly investigated by many scientists (Billard 1984; Gayral and Haas 1969; Loiseaux 1967; Loiseaux and West 1970; O'Kelly 1989; O'Kelly and Floyd 1985); however, the organism (or organisms?) have not been examined using molecular phylogenetic analyses. The organism needs a validly published name and further study, but these are beyond the scope of this paper. Other marine genera, such as *Chrysonephos* (Taylor 1951, 1952), *Nematochryopsis* (Chadefaud 1947; Feldmann 1941) and *Rhamnocrhysis* (Wilce and Markey 1974), also require further study.

### Origin of multicellularity

The phylogenetic tree(s) presented here suggest that the multicellular brown algae (class Phaeophyceae) evolved as a branch after the motile Raphidophyceae and within the poorly resolved clade of the Aurearenophyceae, Chrysoparadoxophyceae, Phaeosacciophyceae, Phaeothamniophyceae and Xanthophyceae. Despite advances made in recent studies (e.g., Cock et al. 2010; Derelle et al. 2017; Graf et al. 2020; Kai et al. 2008; Wetherbee et al. 2019; Yang et al. 2012) we still have a poor understanding of the origin of multicellularity in heterokont algae. One might assume that the ancestors of the brown algae formed cell walls by desmoschisis (cell division where the parent cell wall forms part of the progeny cell wall), rather than the shedding of old mother cell walls by eleuteroschisis (cell division where the progeny cell wall is entirely newly formed) common in the Aurearenophyceae, Chrysoparadoxophyceae and Phaeothamniophyceae. If so, the Phaeosacciophyceae, described here, may be the most likely class to be related to the ancestor of the brown algae. However, despite improvements, the backbone of the SI clade remained unresolved in the phylogenetic trees reported here. Therefore, any further discussion on deep evolutionary events remains in the domain of the hypothetical. In the future, phylogenomic analysis including wide range

of SI clade taxa might resolve the branching order within this clade and help deepening our understanding of the evolution of its multicellularity.

## Methods

### Origin of organisms

*Phaeosaccion collinsii* was collected as an epiphyte of *Zostera marina* from its type locality, Little Nahant, Massachusetts, USA on 24 March 2011 by Kylla M. Benes (42° 25' 58" N, 70° 56' 16" W). Culture strain A12,843 was established on 28 March 2011 by Robert A. Andersen by placing a plant in L1 Medium (Guillard and Hargraves 1993) and adding germanium dioxide to kill the attached diatoms. This unialgal culture was used for DNA extraction. *Antarctosaccion applanatum* was collected from Adelaide Island, Antarctica, on 31 December 2010 by Frithjof Küpper, which is near the type localities of Deception Island and Wiencke Island, Antarctica (Mystikou et al. 2014). A piece of the lectotype specimen of *Tetrasporopsis fuscescens* was taken from 0502-1, Kützing Herbarium, Leiden, The Netherlands (originally collected by A. Braun, Nov. 1846) (see Entwisle and Andersen 1990). *Tetrasporopsis fuscescens* strain SAG 20.88 was obtained from the SAG Culture Collection of Algae, Universität Göttingen University, Germany. *Tetrasporopsis moei* strain A12,475 was collected on 19 June 2010 from a small pool, Northern Michigan USA (47° 14' 03.5"N 88° 25' 33.6"W) by Jason K. Oyadomari and Robert A. Andersen. The alga was isolated from an agar streak plate into unialgal culture on 5 July 2010 by Robert A. Andersen. *Psammocrhysis cassio-tisii* was collected from a high intertidal pool in Narooma Inlet, New South Wales, AUS (36° 12' 27.8"S 150° 07' 30.5"E) by Richard Wetherbee in April 2015. *Nematochrysis sessilis* var. *vectensis* was collected on 27 August 2015 from East Harbour Lagoon, Bembridge (type locality), Isle of Wight, UK (50° 41' 24.0"N 1° 05' 52.4"W) by Roger Herbert and Louis Graf. Culture strain A14,479 was established on 21 September 2015 by micropipette, and after repeated streaking on either h/2 or L1 + NH<sub>4</sub><sup>+</sup> agar plates, strains A14,625-628 were re-isolated by Robert A. Andersen on 13 December 2015. For other microalgae, reference organisms were obtained from public culture collections and grown according to the recommendations provided by the culture collections (Supplementary Material Table S1). Strains not obtained from public culture are available upon request.



## Culturing

The freshwater species were grown in either DY-V medium or a biphasic soil-water medium, and most marine species were grown in L1 or h/2 media (Andersen et al. 2005). Most observations were made from liquid cultures using 20 mm diameter glass test tubes incubated at room temperature with cool-white fluorescent lights (temperature varied from 5–25 °C). *Psammochrysis cassiotisii* was grown on K medium (Andersen et al. 2005) in 60 ml plastic containers at 21 °C and illuminated with Sylvania 58 Luxline Plus and Gro-Lux fluorescent lamps using a 10:14 h light:dark cycle.

## Light microscopy

Most light microscopic observations were made using a Leica DMRB light microscope equipped with differential interference contrast (DIC), phase contrast, brightfield and darkfield optics (Leica Microsystems, <http://www.leica-microsystems.com/home/>, Wetzlar, Germany). Photographs and videos were taken with a Canon EOS T6i Rebel digital single lens reflex camera (Canon USA, Inc, <https://www.usa.canon.com/internet/portal/us/home>). Images were captured as raw files and converted to tagged image file (TIF) documents using the Canon Digital Photo Professional software. Images were further processed and assembled using Adobe Photoshop (Adobe Systems Inc. 2017). For *Psammochrysis*, observations were made using a Zeiss AxioPlan 2 microscope (Carl Zeiss, Oberkochen, Germany) and photographs were taken using a Canon EOS 60D digital single-lens reflex camera (Canon USA, Melville, New York, USA).

***Tetrasporopsis* lectotype material examination:** Genomic DNA was extracted from a 3 mm<sup>2</sup> that was rehydrated in a solution of CTAB buffer + 0.5% β-mercaptoethanol for 1 h at 55 °C before being ground with a pestle. The DNA was from the CTAB solution with 1 V of chloroform and precipitated with 0.5 V of iced isopropanol and 0.09 V of sodium acetate. The DNA was washed with increasingly concentrated ethanol solutions (70% to 95%) before being finally rehydrated in RNase free H<sub>2</sub>O. The extracted genomic DNA was submitted to a whole genome amplification using the Repli-G Mini kit (Qiagen Hilden, Germany) following manufacturer's instructions. The amplified genome was sequenced on the Novaseq6000 platform (Illumina, San Diego, CA USA) producing a total of 62,575,241 paired-end reads that were trimmed for quality and adapter sequence

using Trimmomatic (Bolger et al. 2014) with the following parameters leading:5, trailing:5, sliding window:4:15, and minlen:30. Cleaned reads were mapped on the plastid genome of *Tetrasporopsis fuscescens* SAG 20.88 (unpublished data) and reads mapped on the *atpB*, *psaA*, *psaB*, *psbC* and *rbcL* CDS were recovered and added to respective alignments of publicly available sequences covering the diversity of the heterokont algae and as outgroup sequences of the haptophyte, cryptophyte, rhodophyte and Viridiplantae. Maximum likelihood reconstructions were conducted with IQ-Tree v1.6.12 (Nguyen et al. 2015) with independent substitution model for each partition determined with the -m MFP option and branch supports were obtained with the ultrafast bootstrap (UFBoot) with 5000 replications and non-parametric bootstrapping (BP) with 250 replications both implemented in IQ-Tree (Hoang et al. 2018).

## DNA extraction, amplification and sequencing

Genomic DNA was extracted from each culture strain using either the DNeasy Plant Mini Kit (Qiagen, Hilden, Germany) or the Tissue Miniprep Kit (Cosmo Genetech, Seoul, Korea) according to the manufacturer's instructions. PCR and sequencing were performed using various combinations of published primers (Bailey et al. 1998; Daugbjerg and Andersen 1997; Yang et al. 2012; Yoon et al. 2002). PCR amplifications were performed on a total volume of 20 μl. PCR mix of 1 μl of each primers and 5–50 ng of template DNA were added to the AccuPower PCR Premix (Bioneer, Daejeon, Korea) containing 1U *Top DNA polymerase*, 250 μM of each dNTPs, 10 mM of Tris-HCl (pH 9.0), 30 mM of KCl and 1.5 mM of MgCl<sub>2</sub>. Standard cycling parameters were an initial denaturation at 95 °C for 5 min, 35 main amplification cycles of denaturation at 95 °C for 30 s, annealing at 40–55 °C depending on the primer set for 30 s, and elongation at 72 °C for 30 s, followed by a final elongation at 72 °C for 10 min. Post-cycling, samples were held at 4 °C.

PCR products were loaded onto a 0.8% standard agarose gel for electrophoresis (15–25 min at 200 V). Unsuccessfully amplified samples were subjected to multiple amplifications at various template DNA and/or MgCl<sub>2</sub> concentrations. Amplified DNA was purified with the PCR purification Kit (Cosmo Genetech, Seoul, Korea) and sent to Macrogen Inc. (Seoul, Korea) for forward and reverse sequencing. Electropherogram outputs for each specimens were carefully read and edited if necessary using the program 4Peaks version

1379 1.7.2 (<http://nucleobytes.com/index.php/4peaks>)  
 1380 finally forward and reverse sequences  
 1381 were combined using Se-AL version 2.0a11  
 1382 (<http://tree.bio.ed.ac.uk/software/seal/>). Newly  
 1383 determined sequences were deposited in  
 1384 the GenBank (<http://www.ncbi.nlm.nih.gov>)  
 1385 databases under the accession number  
 1386 MT581941-MT582138 Data ready for submission.

### 1387 Phylogenetic analyses

1388 Published sequences were obtained from Gen-  
 1389 Bank and aligned using MAFFT version 6 using  
 1390 the G-INS-i strategy and with an offset value of  
 1391 0.1 (Kato et al. 2002) and subsequently care-  
 1392 fully refined manually using Se-AL version 2.0a11  
 1393 (<http://tree.bio.ed.ac.uk/software/seal/>). In order to  
 1394 reduce the tree constructions artifacts, only unam-  
 1395 biguous regions of the nuclear SSU rRNA were  
 1396 used. The nuclear SSU rRNA positions (reference  
 1397 *Nannochloropsis granulata* U41092) that were  
 1398 used in the analyses are: 1–67, 75–127, 132–172,  
 1399 181–232, 237–239, 243–276, 289–641, 717–732,  
 1400 742–824, 833–1061, 1068–1353, 1361–1367,  
 1401 1382–1495, 1502–1689, 1718–1792. Any ambigu-  
 1402 ous positions (e.g., N) were treated as missing  
 1403 during the subsequent analyses. In most cases the  
 1404 same strain was used when determining all gene  
 1405 sequences. However, as the five genes dataset  
 1406 (SSU rRNA, *rbcL*, *psaA*, *psaB*, *atpB*) was designed  
 1407 to minimize the effect of missing data in the con-  
 1408 catenated alignment on phylogeny, we combined  
 1409 publicly available sequences from different strains  
 1410 in one case for ingroup species (Supplementary  
 1411 Material Table S1). The five gene alignments were  
 1412 concatenated into one dataset using SequenceMa-  
 1413 trix 1.7.6 (Vaidya et al. 2011) where each gene  
 1414 represented a partition. Maximum likelihood recon-  
 1415 structions were conducted with IQ-Tree v1.6.12  
 1416 (Nguyen et al. 2015) with independent substi-  
 1417 tution model for each partition determined with  
 1418 the-m MFP option. They were the General Time  
 1419 Reversible (GTR; Tavaré 1986) with a 4-class  
 1420 gamma distributed rate heterogeneity (G4) with  
 1421 empirical base frequencies (F) and invariable sites  
 1422 (I) for *atpB*, *psaB* and *psbA*; the GTR with a 5-class  
 1423 FreeRate model (R5; Soubrier et al. 2012) with  
 1424 empirical base frequencies for *psaA*, *psbC* and *rbcL*  
 1425 and the TN (Tamura and Nei 1993) with a 7-class  
 1426 FreeRate model (R7) with empirical base frequen-  
 1427 cies (F) for the nuclear SSU. For the amino acid the  
 1428 evolutionary model were the mitochondrial meta-  
 1429 zoa (mtZOA; Rota-Stabelli et al. 2009) with G4 and I  
 1430 for *psbA*; the mtZOA with R4 for the *psaA* and *psbC*;  
 1431 the General Matrix (LG; Le and Gascuel 2008) with

R4 for the *psaB* and *rbcL* and the chloroplast matrix  
 (cpREV; Adachi et al. 2000) with G4 and I for *atpB*.  
 Branch supports were obtained with the ultrafast  
 bootstrap (UFBoot) with 5000 replications and non-  
 parametric bootstrapping (BP) with 250 replications  
 both implemented in IQ-Tree (Hoang et al. 2018).

### Author contributions

L.G., R.A.A. and H.S.Y. designed the project. L.G.,  
 F.C.K., K.M.B., J.K.O., R.J.H.H., H.V., R.W., and  
 R.A.A. collected the samples. L.G., E.C.Y., K.Y.H.,  
 and H.V., conducted the experiments (DNA extrac-  
 tions and PCR). L.G., H.V., R.A.A., and H.S.Y.  
 analyzed and interpreted the data. L.G., H.V., R.W.,  
 R.A.A., and H.S.Y. wrote the draft and all authors  
 read the manuscript.

### Conflicts of interest

We are submitting a revised manuscript entitled,  
 “Multigene phylogeny, morphological observation  
 and re-examination of the literature lead to the  
 description of the Phaeosacciophyceae *classis*  
*nova* and four new species of the Heterokontophyta  
 SI Clade” for consideration as a research article in  
*Protist*. All authors have approved the revisions of  
 the paper, the results are unpublished and contents  
 have not been submitted for publication elsewhere.  
 All the authors declare no conflicts of interest.

### Acknowledgements

The authors are very grateful to Richard Moe  
 (University of California-Berkeley) for help with  
 Latin names and nomenclatural questions; to  
 John McNeill (Royal Botanic Garden, Edinburgh)  
 for help with applications of the ICN; to Donald  
 Pfister (Farlow Herbarium, Harvard University)  
 for help locating the original material studied by  
 Farlow (1882); to Michael Wynne (University of  
 Michigan) and Craig Schneider (Trinity College,  
 Connecticut) for help with the *Phaeosaccion* litera-  
 ture. This work was supported by the Collaborative  
 Genome Program of the Korea Institute of Marine  
 Science and Technology Promotion (KIMST)  
 funded by the Ministry of Oceans and Fish-  
 eries (MOF) (20180430), the National Research  
 Foundation of Korea (NRF-2017R1A2B3001923,  
 2020R1C1C1008173), the Next-generation  
 BioGreen21 Program (PJ01389003) from the  
 RDA (Rural Development Administration), Korea

and National Science Foundation (DEB-0936884, 1317114) to H.S.Y. Support was provided by the National Science Foundation (DEB-9419498, EF 08-27023) to R.A.A. We would equally like to thank the UK Natural Environment Research Council for their support to F.C.K. (program Oceans 2025 – WP 4.5 and grants NE/D521522/1, NE/J023094/1 and, for the expedition to Antarctica, CGS-70). This work also received support from the Marine Alliance for Science and Technology for Scotland pooling initiative. MASTS is funded by the Scottish Funding Council (grant reference HR09011) and contributing institutions.

## Appendix A. Supplementary data

Supplementary data associated with this article can be found, in the online version, at doi:10.1016/j.protis.2020.125781.

## References

- Adachi J, Waddell PJ, Martin W, Hasegawa M (2000) Plastid genome phylogeny and a model of amino acid substitution for proteins encoded by chloroplast DNA. *J Mol Evol* **50**:348–358
- Andersen RA, Berges J, Harrison P, Watanabe M (2005) Recipes for freshwater and seawater media. In Andersen RA (ed) *Algal culturing techniques*. Elsevier/Academic, Burlington, MA, pp 429–532
- Andersen RA, Potter D, Bidigare RR, Latasa M, Rowan K, O’Kelly CJ (1998) Characterization and phylogenetic position of the enigmatic golden alga *Phaeothamnion confervicola*: ultrastructure, pigment composition and partial SSU rDNA sequence. *J Phycol* **34**:286–298
- Bailey JC, Bidigare RR, Christensen SJ, Andersen RA (1998) Phaeothamniophyceae classis nova: a new lineage of chromophytes based upon photosynthetic pigments, *rbcL* sequence analysis and ultrastructure. *Protist* **149**:245–263
- Billard C (1984) Ph. D. thesis Recherches sur les Chrysophyceae marines de l’ordre des Sarcinochrysidales. Biologie, systématique, phylogénie Ph.D. thesis. Université de Caen, 224 pp.
- Bolger AM, Lohse M, Usadel B (2014) Trimmomatic: a flexible trimmer for Illumina sequence data. *Bioinform* **30**:2114–2120
- Bourelly P (1957) Recherches sur les Chrysophycées. Morphologie, phylogénie, systématique. *Rev Algol Mém Hors Sér* **1**:1–412
- Broom JE, Jones WA, Nelson WA, Farr TJ (1999) A new record of a marine macroalga from New Zealand – *Giraudyopsis stellifera*. *N Z J Bot* **37**:751–753
- Carter N (1937) New or interesting algae from brackish water. *Arch Protistenkd* **90**:1–68
- Cavalier-Smith T, Chao EE, Aillsopp MTEP (1995) Ribosomal RNA evidence for chloroplast loss within Heterokonta: pedinellid relationships and a revised classification of ochristan algae. *Arch Protistenkd* **145**:209–220
- Chadefaud M (1947) Une nouvelle Chrysophycée marine filamenteuse: *Nematochryopsis roscoffensis* n. g. n. sp. *Bull Soc Bot France* **94**:239–243
- Chen LC-M, McLachlan J, Craigie JS (1974) The fine structure of the marine chrysophycean alga *Phaeosaccion collinsii*. *Can J Bot* **52**:1621–1624
- Cock JM, Sterck L, Rouzé P, Scornet D, Allen AE, Amoutzias G, Anthouard V, Artiguenave F, Aury J-M, Badger JH, Beszteri B, Billiau K, Bonnet E, Bothwell JHF, Bowler C, Boyen C, Brownlee C, Carrano CJ, Charrier B, Cho GY, Coelho SM, Collén J, Corre E, Da Silva C, Delage L, Delaroque N, Dittami SM, Doubeau S, Elias M, Farnham G, Gachon CMM, Gschloessl B, Heesch S, Jabbari K, Jubin C, Kawai H, Kimura K, Kloareg B, Küpper FC, Lang D, Le Bail A, Leblanc C, Lerouge P, Lohr M, Lopez PJ, Martens C, Maumus F, Michel G, Miranda-Saavedra D, Morales J, Moreau H, Motomura T, Nagasato C, Napoli CA, Nelson DR, Nyvall-Collén P, Peters AF, Pommier C, Potin P, Poulain P, Quesneville H, Read B, Rensing SA, Ritter A, Rousvoal S, Samanta M, Samson G, Schroeder DC, Ségurens B, Strittmatter M, Tonon T, Tregear J, Valentin K, von Dassow P, Yamagishi T, Van de Peer Y, Wincker P (2010) The *Ectocarpus* genome and the independent evolution of multicellularity in brown algae. *Nature* **465**:617–621
- Cryan AE, Benes KM, Gillis B, Ramsay-Newton C, Perini V, Wynne MJ (2015) Growth, reproduction, and senescence of the epiphytic marine alga *Phaeosaccion collinsii* Farlow (Ochrophyta, Phaeothamniales) at its type locality in Nahant, Massachusetts, USA. *Bot Mar* **58**:275–283
- Delépine R, Lamb IM, Zimmermann M (1970) Sur les algues marines antarctiques rapportées au genre *Monostroma* Thuret. *Compt Rend Acad Sc Paris, sér D* **270**:1973–1976
- Derelle R, Lopez-Garcia P, Timpano H, Moreira D (2016) A phylogenetic framework to study the diversity and evolution of stamenopiles (=heterokonts). *Mol Biol Evol* **33**:2890–2898
- Dangard P (1965) Sur un nouveau genre de Phéophycées: *Giraudyopsis* nov. gen.(*Giraudyopsis stellifer* nov. sp.). *Compt Rend Acad Sci Paris, sér D* **261**:2699–2701, +2 plates
- Dangard P (1966) Sur le nouveau genre *Giraudyopsis* P. D. *Botaniste* **49**:99–108
- Daugbjerg N, Andersen RA (1997) A molecular phylogeny of the heterokont algae based on analyses of chloroplast-encoded *rbcL* sequence data. *J Phycol* **33**:1031–1041
- De Toni JB (1895) *Sylogae Algarum*. Vol. 3. Fucoideae (privately published) Padova, xvi-638 p.
- Entwistle TJ, Andersen RA (1990) A re-examination of *Tetrasporopsis* (Chrysophyceae) and the description of *Dermatochrysis* gen. nov (Chrysophyceae): a monostromatic alga lacking cell walls. *Phycologia* **29**:263–274
- Ettl H (1966) *Phaeobotrys solitaria*, eine neue coccale Chrysophyceae. *Rev Algol N S* **8**:211–214
- Farlow WG (1882) Notes on New England algae. *Bull Torrey Bot Club* **9**:65–68
- Feldmann J (1941) Une nouvelle Xanthophycée marine: *Tribonema marinum* nov. sp. *Bull Soc d’Hist Nat l’Afrique du Nord Algiers* **32**:56–61



- 1586 **Gain ML** (1911) Note sur trois espèces nouvelles d'algues marines provenant de la région Antarctique Sud-Américaine. Bull Mus Natl Hist Nat [Paris] **17**:482–484 1641
- 1587 1642
- 1588
- 1589 **Gabrielson PW, Lindstrom SC** (2018) Keys to the seaweeds and seagrasses of southeast Alaska, British Columbia Washington and Oregon. Phycological Contribution **9**:1–180 1644
- 1590 1645
- 1591
- 1592 **Gayral P, Billard C** (1977a) Synopsis du nouvel ordre des Sarcinochrysidales (Chrysophyceae). Taxon **26**:241–245 1646
- 1593 1647
- 1594 **Gayral P, Billard C** (1977b) Chrysophycées et Haptophycées 1648
- 1595 des côtes françaises: mise au point systématique et nouvelles observations sur *Ruttnera chadefaudii* Bourrelly et Magne 1649
- 1596 (Haptophycées). Bull Soc Phycol de France **22**:135–149 1650
- 1597 1651
- 1598 **Gayral P, Haas C** (1969) Étude comparée des genres 1652
- 1599 *Chrysomeris* Carter et *Giraudyopsis* P Dang. position systématique des Chrysomeridaceae (Chrysophyceae). Rev Gen Bot **76**:659–666 1653
- 1600 1654
- 1601 1655
- 1602 **Gayral P, Lepailleur H** (1971) Étude de deux Chrysophycées 1656
- 1603 filamenteuses: *Nematochryopsis roscoffensis* Chadefaud, 1657
- 1604 *Nematochrysis hieroglyphica* Waern. Rev Gen Bot **78**:61–74 1658
- 1605 1659
- 1606 **Graf L, Yang EC, Boo GH, Andersen RA, Yoon HS** (2020) 1660
- 1607 Further investigations of the Phaeothamniophyceae using a 1661
- 1608 multigene phylogeny, with descriptions of five new species. J 1662
- 1609 Phycol **56**:358–379 1663
- 1610 1664
- 1611 **Guillard RRL, Hargraves PE** (1993) *Stichochrysis immobilis* 1665
- 1612 is a diatom, not a chrysophyte. Phycologia **32**:234–236 1666
- 1613 1667
- 1614 **Han KY, Graf L, Reyes CP, Melkonian B, Andersen RA, 1668**
- 1615 **Yoon HS, Melkonian M** (2018) A re-investigation of *Sarcinochrysis marina* (Sarcinochrysidales, Pelagophyceae) from its type locality and the descriptions of *Arachnochrysis*, *Pelagospilus*, *Sargassococcus* and *Sungminbooa* genera nov. Protist **169**:79–106 1669
- 1616 1670
- 1617 **Hoang DT, Chernomor O, von Haeseler A, Minh BQ, Vinh 1671**
- 1618 **LS** (2018) UFBboot2: improving the ultrafast bootstrap approximation. Mol Biol Evol **35**:518–522 1672
- 1619 1673
- 1620 **Kai A, Yoshii Y, Nakayama T, Inouye I** (2008) Aurearenophyceae classis nova, a new class of Heterokontophyta based on a new marine unicellular alga *Aurearena cruciata* gen. et sp. nov. inhabiting sandy beaches. Protist **159**:435–457 1674
- 1621 1675
- 1622 1676
- 1623 1677
- 1624 **Katoh K, Misawa K, Kuma K, Miyata T** (2002) MAFFT: a novel 1678
- 1625 method for rapid multiple sequence alignment based on fast 1679
- 1626 Fourier transform. Nucleic Acids Res **30**:3059–3066 1680
- 1627 1681
- 1628 **Kützing FT** (1849) Species Algarum. F.A. Brockhaus, Leipzig. p. 922 p 1682
- 1629 1683
- 1630 **Kjellman FR** (1891) Phaeophyceae (Fucoideae). In Engler 1684
- 1631 A, Prantl K (eds) Die Natürlichen Pflanzenfamilien. I. Teil. 2, Leipzig, pp 176–192 1685
- 1632 1686
- 1633 **Le SQ, Gascuel O** (2008) An improved general amino acid 1687
- 1634 replacement matrix. Mol Biol Evol **25**:1307–1320 1688
- 1635 1689
- 1636 **Lemmermann E** (1899) Das Phytoplankton sächsischer 1690
- 1637 Teiche. Forschungsberichte aus der Biologischen Station zu 1691
- 1638 Plön **7**:96–135 1692
- 1639 1693
- 1640 **Loiseaux S** (1967) Sur la position Systématique du genre 1694
- Giraudyopsis* P. Dangeard. Rev Gen Bot **74**:389–395, +2 plates 1695
- 1696
- Loiseaux S, West JA** (1970) Brown algal mastigonemes: comparative ultrastructure. Trans Am Microsc Soc **89**:524–532 1697
- Mathieson AC, Dawes CJ** (2017) Seaweeds of the Northwest Atlantic. Univ Mass Press, Amhurst, 798 p 1698
- McLachlan J, Chen LC-M, Edelman T, Craigie JS** (1971) Observations on *Phaeosaccion collinsii* in culture. Can J Bot **49**:563–566 1699
- Mystikou A, Peters AF, Asensi AO, Fletcher KI, Brickle P, van West P, Convey P, Küpper FC** (2014) Seaweed biodiversity in the south-western Antarctic Peninsula: Surveying macroalgal community composition in the Adelaide Island/Marguerite Bay region over a 35-year time span. Polar Biology **37**:1607–1619 1700
- Nguyen L-T, Schmidt HA, von Haeseler A, Minh BQ** (2015) IQ-TREE: a fast and effective stochastic algorithm for estimating maximum-likelihood phylogenies. Mol Biol Evol **32**:268–274 1701
- O'Kelly CJ** (1989) The Evolutionary Origin of the Brown Algae: Information from Studies of Motile Cell Structure. In Green JC, Leadbeater BSC, Diver WL (eds) The Chromophyte Algae: Problems and Perspectives. Syst Assoc Spec Vol 38. Clarendon Press, Oxford, pp 255–278 1702
- O'Kelly CJ, Floyd GL** (1985) Absolute configuration analysis of the flagellar apparatus in *Giraudyopsis stellifer* (Chrysophyceae Sarcinochrysidales) zoospores and its significance in the evolution of the Phaeophyceae. Phycologia **24**:263–274 1703
- Pascher A** (1914a) Über Flagellaten und Algen. Ber Deutsch Bot Ges **32**:136–160 1704
- Pascher A** (1914b) Zur Notiz über Flagellaten und Algen. Ber Deutsch Bot Ges **32**:430 1705
- Pascher A** (1925) Die braune Algenreihe der Chrysophyceen. Arch Protistenkd **52**:489–564 1706
- Pascher A** (1939) Heterokonten. In Rabenhorst L (ed) Kryptogamen-Flora von Deutschland, Österreich und der Schweiz. Lieferung 2, Band XI. Akademische Verlagsgesellschaft, Leipzig, pp 1092 p 1707
- Rota-Stabelli O, Yang Z, Telford MJ** (2009) MtZoa: a general mitochondrial amino acid substitutions model for animal evolutionary studies. Mol Phylogenet Evol **52**:268–272 1708
- Saunders GW, Potter D, Andersen RA** (1997) Phylogenetic affinities of the Sarcinochrysidales and Chrysomeridales (Heterokonta) based on analyses of molecular and combined data. J Phycol **33**:310–318 1709
- Schussnig B** (1940) Über einige neue Protophyten aus der Adria. Arch Protistenkd **93**:317–330 1710
- Soubrier J, Steel M, Lee MSY, Der Sarkissian C, Guindon S, Ho SYW, Cooper A** (2012) The influence of rate heterogeneity among sites on the time dependence of molecular rates. Mol Biol Evol **29**:3345–3358 1711
- Stancheva R, Škaloud P, Pusztai M, Loflen CL, Sheath RG** (2019) First record of the rare freshwater alga *Tetrasporopsis fuscescens* Chrysomerophyceae Ochrophyta in North America. Fottea **19**:163–174 1712
- Starmach K** (1985) Chrysophyceae und Haptophyceae. In Ettl H, Gerloff J, Heynig H, Mollenhauer D (eds) Süßwasserflora von Mitteleuropa, Band 1. Gustav Fischer Verlag, Stuttgart Germany, 515 p 1713

- 1697 **Tamura N, Nei M** (1993) Estimation of the number of nucleotide  
1698 substitutions in the control region of mitochondrial DNA in  
1699 humans and chimpanzees. *Mol Biol Evol* **10**:512–526
- 1700 **Tavare S** (1986) Probabilistic and statistical problems in the  
1701 analysis of DNA Sequences. In Miura RM (ed) *Some mathe-*  
1702 *matical questions in biology DNA sequence analysis*. Am Math  
1703 Soc, Providence (USA), pp 57–86
- 1704 **Taylor WR** (1951) Structure and reproduction of  
1705 *Chrysosphaeum lewisii*. *Hydrobiologia* **3**:122–130
- 1706 **Taylor WR** (1952) The algal genus *Chrysosphaeum*. *Bull Torrey*  
1707 *Bot Club* **79**:79
- 1708 **Turland NJ, Wiersema JH, Barrie FR, Greuter W,**  
1709 **Hawksworth PS, Herendeen PS, Knapp S, Kusber W-H, Li**  
1710 **D-Z, Marhold K, May TW, McNeill J, Monro AM, Prado J,**  
1711 **Price MJ, Smith GF** (2018) International code of nomencla-  
1712 *ture for algae, fungi and plants* (Shenzhen Code). *Reg Veg*  
1713 **159**:1–254
- 1714 **Vaidya G, Lohman DJ, Meier R** (2011) SequenceMatrix:  
1715 concatenation software for the fast assembly of multi-gene  
1716 datasets with character set and codon information. *Cladistics*  
1717 **27**:171–180
- 1718 **Waern M** (1952) PhD thesis Rocky-shore algae in the Öregrund  
Archipelago PhD thesis. Univ Uppsala, Sweden
- West W, West GS** (1903) Notes on freshwater algae. III. *J Bot*  
*Br Foreign* **41**:33–41
- Wetherbee R, Gornik SG, Grant B, Waller R** (2015) *Anderse-*  
*nia*, a genus of filamentous, sand-dwelling Pelagophyceae from  
southeastern Australia. *Phycologia* **54**:35–48
- Wetherbee R, Jackson CJ, Repetti SI, Clementson LA,**  
**Costa JF, van de Meene A, Crawford S, Verbruggen H** (2019)  
The golden paradox – a new heterokont lineage with chloro-  
plasts surrounded by two membranes. *J Phycol* **55**:257–278
- Wilce RT, Markey DR** (1974) *Rhamnocrhysis aestuarinae*: a  
new monotypic genus of the benthic marine chrysophytes. *J*  
*Phycol* **10**:82–88
- Wynne MJ, Furani G** (2014) A census of J. P.L Dangeard's  
invalid taxa with proposals to resolve the nomenclatural prob-  
lems of some of them. *Nov Hedw* **98**:515–527
- Yang EC, Boo GH, Kim HJ, Cho SM, Boo SM, Andersen**  
**RA, Yoon HS** (2012) Supermatrix data highlight the phyloge-  
netic relationships of the photosynthetic stramenopiles. *Protist*  
**163**:217–233
- Yoon HS, Hackett JD, Bhattacharya D** (2002) A single origin  
of the peridinin-and fucoxanthin-containing plastids in dinoflag-  
ellates through tertiary endosymbiosis. *Proc Natl Acad Sci USA*  
**99**:11724–11729

Available online at [www.sciencedirect.com](http://www.sciencedirect.com)

ScienceDirect